

# POLITECNICO DI TORINO

Master Course in Aerospace Engineering

Master's Degree Thesis

## Fiber Bragg Grating Sensors for Mechanical and Thermal Prognostics and Diagnostics for Aerospace Applications



Supervisor:  
Prof. Paolo Maggiore

Co-Supervisors:  
Prof. Daniel Milanese  
Prof. Davide Luca Janner  
Ing. Matteo Dalla Vedova

Candidate:  
Giancarlo Candiano

20 July 2018



# Summary

This work, developed at the *Department of Mechanical and Aerospace Engineering* (DIMEAS) of the Politecnico di Torino in collaboration with the interdepartmental center *Photonext* and the *Istituto Superiore Mario Boella* (ISMB), concerns the study of innovative fiber optic sensors as well as Fiber Bragg Grating (FBG) sensors. These sensors have many advantages compared to the traditional sensors. In fact, they are lighter and smaller, they do not need of an external power supply and they are immune to electromagnetic interference and to harsh environment. Moreover, one of the most important advantages is the possibility to have dozens of sensors inside the same fiber optic and each sensor can detect a particular physical quantity such as strain, temperature, pressure and vibration.

The future aim is to use these sensors for prognostic and diagnostic activities in Aerospace applications.

The objectives of this work are the study of these optical sensors and the assembly of a test bench aimed at the study of FBGs and of performances of locking systems designed and manufactured to lock the fiber optic to the structure. This work was divided into three phases. The first phase involved the design and implementation of different types of locking systems used in mechanical and thermal tests. In particular, for the mechanical tests, locking systems have been designed in order to allow the use of a rubber layer to lock the optical fiber and this system turns out to be a system that is easy to manufacture and re-usable, even in case of breakage of the optical fiber itself. Another locking system for mechanical tests is based on the gluing of the fiber. This type of system will turn out to be the best locking system and, although in particular situation it is difficult to reuse it if fiber optic breaks, it guarantees the best results in terms of wavelength, strain or displacements detected by the optical sensors used by us. Therefore, also for the thermal tests two concepts of systems have been realised to lock the fiber. In the second phase of this work, the assembly of a test bench took place. In the third and last phase, the measurement campaigns have been done in order to allow us to test the FBG sensors and locking systems.

Moreover, these measurement campaigns allowed us to study all the positive and negative aspects of the different locking systems and the optical fiber sensors.

# Sommario

Questo lavoro di Tesi, svolto presso il *Dipartimento di Ingegneria Meccanica e Aerospaziale* (DIMEAS) del Politecnico di Torino in collaborazione con il centro interdipartimentale *Photonext* e l'*Istituto Superiore Mario Boella* (ISMB), riguarda lo studio di sensori innovativi in fibra ottica nonché i sensori a reticolo di Bragg (FBG). Questi sensori hanno molti vantaggi rispetto ai sensori tradizionali. Infatti, sono leggeri e di piccole dimensioni, non necessitano di alimentazione elettrica, sono immuni alle interferenze elettromagnetiche, agli *harsh environments*. Inoltre, uno dei vantaggi più importanti è la possibilità di avere all'interno di un'unica fibra ottica decine di sensori e ciascun sensore può rilevare una grandezza fisica differente come strain, temperatura, pressione e vibrazione.

L'idea futura è di utilizzare questi sensori per attività di prognostica e diagnostica in applicazioni Aerospaziali.

Gli obiettivi di questo lavoro sono lo studio di questi sensori ottici e la realizzazione di un banco prova finalizzato allo studio degli FBG e delle performance dei sistemi di bloccaggio progettati e realizzati per bloccare la fibra alla struttura.

Il lavoro è stato suddiviso in tre fasi. Nella prima fase ha avuto luogo la progettazione e la realizzazione di diversi sistemi di bloccaggio da utilizzare nelle prove meccaniche e termiche. In particolare, per le prove meccaniche sono stati realizzati sistemi di bloccaggio che permettono l'utilizzo di un layer in gomma per il bloccaggio della fibra e questi risultano essere dei sistemi di facile realizzazione e riutilizzabili anche in caso di rottura della fibra ottica. Un'altra tipologia di sistema di bloccaggio è basata sull'incollaggio della fibra. Quest'ultimo sistema risulterà essere il migliore perché, nonostante in particolari situazioni sia di difficile riutilizzo nel caso di rottura della fibra ottica, garantisce i migliori risultati in termini di lunghezze d'onda, deformazioni o spostamenti rilevati dai sensori ottici utilizzati. In ultimo, anche per le prove termiche sono stati realizzati due differenti concept di sistemi per bloccare la fibra ottica. Nella seconda fase di questo lavoro ha avuto luogo l'assemblaggio del banco prova e nella terza e ultima fase hanno avuto luogo le campagne di misurazione che ci hanno permesso di testare non solo i sensori FBG ma anche i sistemi

di bloccaggio.

Inoltre, i test eseguiti ci hanno permesso di studiare tutti gli aspetti positivi e negativi dei diversi sistemi di bloccaggio e della fibra stessa.

# Acknowledgements

I would like to thank all people who helped and supported me during my this important Academic career and all people with whom i collaborated during this important research project. In particular, I would like to thank my supervisor Professor Paolo Maggiore, who has guided me during this research project and i really admire his immense knowledge and availability to all of us students. Moreover, my sincere thanks to Ing. Matteo Dalla Vedova, Professor Davide Luca Janner and Professor Daniel Milanese for their great support for carrying out the research work. In addition, I would like to thank all my colleagues and friends who supported me during these years and making this experience unique. I also want to thank my girlfriend Chiara for supporting me and giving me strength in everything.

At the end, an immense and immeasurable thanks to my parents for all the sacrifices they made during this years, giving me the opportunity to study. They have always been present in all my positive and negative moments, supporting and advising me always. A sincere and immense thanks to Giovanni and Adelia.

# Table of contents

|   |           |
|---|-----------|
| <b>Summary</b>  | I         |
| <b>Sommario</b>   | III       |
| <b>Acknowledgements</b>   | V         |
| <b>List of figures</b>  | X         |
| <b>List of tables</b>   | XI        |
| <b>1 Introduction</b>   | <b>1</b>  |
| 1.1 Objectives . . . . .  | 2         |
| 1.2 Thesis structure . . . . .                                      | 2         |
| <b>2 Fiber Optic and Optical Fiber Sensors</b>                      | <b>4</b>  |
| 2.1 Overview of Materials . . . . .                                 | 4         |
| 2.2 Geometry and basic classification of Fiber Optics . . . . .     | 5         |
| 2.3 Physical Principles behind Fiber Optics . . . . .               | 7         |
| 2.4 Advantages and Disadvantages of using the Fiber Optic . . . . . | 9         |
| 2.5 Fiber Bragg Grating Sensors . . . . .                           | 10        |
| 2.5.1 Fundamental equations of FBGs . . . . .                       | 12        |
| <b>3 Assembly of Test Bench</b>                                     | <b>14</b> |
| 3.1 Platform . . . . .  | 14        |
| 3.2 Locking Systems for Mechanical tests . . . . .                  | 16        |
| 3.2.1 Aluminium Locking Systems . . . . .                           | 16        |
| 3.2.2 3D Printed Locking Systems . . . . .                          | 20        |
| 3.3 Locking Systems for Thermal tests . . . . .                     | 23        |
| 3.4 Splicing of Fiber Optics . . . . .                              | 26        |
| 3.5 Interrogation layout . . . . .                                  | 29        |

|          |  |           |
|----------|--|-----------|
| <b>4</b> | <b>Matlab script for the Post processing</b>   | <b>30</b> |
| 4.1      | Structure of the Matlab script . . . . .   | 30        |
| 4.2      | Basic physical principle . . . . .   | 31        |
| 4.3      | Explanation of Matlab script . . . . .   | 31        |
| 4.3.1    | Check of the presence of necessary files . . . . .   | 31        |
| 4.3.2    | Choice of analysis type . . . . .  | 32        |
| 4.3.3    | Setting of FBG sensor . . . . .  | 32        |
| 4.3.4    | Saving data . . . . .  | 33        |
| <b>5</b> | <b>Tests and Measurements</b>  | <b>34</b> |
| 5.1      | Locking system with Hard rubber layer . . . . .  | 35        |
| 5.1.1    | Response in terms of strain and wavelength by using the short<br>line $L_o=53.59$ mm . . . . .                                   | 35        |
| 5.1.2    | Response in terms of strain and wavelength by using the in-<br>termediate line $L_o=128.80$ mm . . . . .                         | 38        |
| 5.1.3    | Response in terms of strain and wavelength by using the long<br>line $L_o=228.94$ mm . . . . .                                   | 41        |
| 5.1.4    | Repeatability test with locking system with Hard rubber . . .  | 43        |
| 5.2      | Locking system with Soft rubber layer . . . . .  | 45        |
| 5.2.1    | Response in terms of strain and wavelength by using the short<br>line $L_o=58.59$ mm and the long line $L_o=228.94$ mm . . . . . | 45        |
| 5.3      | Locking system with Epoxy resin . . . . .  | 49        |
| 5.3.1    | Comparison between two concepts of locking systems . . . . .   | 49        |
| 5.3.2    | Conclusion of comparison between two concepts of locking sys-<br>tems . . . . .  | 56        |
| 5.3.3    | Comparison between two different lines: $L_o=53.59$ mm and<br>$L_o=228.94$ mm . . . . .  | 57        |
| 5.3.4    | Conclusion about the comparison between two different lines $L_o$  | 63        |
| 5.3.5    | Repeatability Test with long line $L_o=228.94$ mm by varying<br>the preload . . . . .  | 63        |
| <b>6</b> | <b>Conclusions and Future works</b>  | <b>66</b> |
|          | <b>References</b>  | <b>68</b> |

# List of figures

|      |  |    |
|------|--|----|
| 2.1  | Example of fiber optic structure. (©2018 Newport Corporation. All rights reserved) . . . . .                             | 5  |
| 2.2  | (a) Single-mode fiber, (b) Multi-mode fiber of step index type, (c) Multi-mode fiber of graded index type. [6] . . . . . | 6  |
| 2.3  | Main angles of a fiber optic. [8] . . . . .  | 8  |
| 2.4  | Summary of the main characteristics of the Fiber Bragg Grating sensors [8]. . . . .                                      | 13 |
| 2.5  | Shift of the wavelength due to an application of a load. . . . .   | 13 |
| 3.1  | Load-Frequency per each passive dumper ( <i>Copyright 1999-2018 Thorlabs, Inc.</i> ). . . . .                            | 15 |
| 3.2  | Optical enclosure ( <i>Copyright 1999-2018 Thorlabs, Inc.</i> ). . . . .   | 15 |
| 3.3  | Package of locking system for mechanical tests. . . . .  | 17 |
| 3.4  | Bottom base mounted on breadboard. . . . .   | 17 |
| 3.5  | Package located on the micro translation stage. . . . .  | 18 |
| 3.6  | Package located directly on the breadboard. . . . .  | 18 |
| 3.7  | V-groove. . . . .  | 19 |
| 3.8  | Set-up for Mechanical tests. . . . .   | 19 |
| 3.9  | Fluttening of the rubber layer. . . . .  | 20 |
| 3.10 | Locking system in Polylactic Acid (PLA). . . . .   | 20 |
| 3.11 | Container for resin. . . . .   | 21 |
| 3.12 | Final manufactured products. . . . .   | 21 |
| 3.13 | Container for resin. . . . .   | 22 |
| 3.14 | Rectangular plate. . . . .   | 22 |
| 3.15 | Set up of Locking systems for resin. . . . .   | 23 |
| 3.16 | Three components of the package for thermal tests. . . . .   | 24 |
| 3.17 | Base for Peltier module. . . . .   | 24 |
| 3.18 | Final package locking system for thermal testing. . . . .  | 25 |
| 3.19 | Two different types of clevers. . . . .  | 26 |

|      |  |    |
|------|--|----|
| 3.20 | Position of fiber optics inside the splicer. . . . .   | 27 |
| 3.21 | Splicing process and estimated loss shown on the monitor. . . . .  | 27 |
| 3.22 | Heat shrinkable tube. . . . .  | 28 |
| 3.23 | Interrogation system . . . . .   | 29 |
| 5.1  | Response in terms of strain ( $\epsilon$ ) and wavelength ( $\lambda$ ) for the short line.                | 36 |
| 5.2  | Detail of fiber optic sliding in terms of strain for the short line. . . . .                               | 37 |
| 5.3  | Experimental and Theoretical curves for locking system with hard rubber and $L_o=53.59$ mm. . . . .        | 38 |
| 5.4  | Response in terms of strain ( $\epsilon$ ) and wavelength ( $\lambda$ ) for the intermediate line. . . . . | 39 |
| 5.5  | Comparison between Theoretical and Experimental curves for the intermediate line. . . . .                  | 39 |
| 5.6  | Detail of fiber optic sliding and rubber deformation in terms of strain for the intermediate line. . . . . | 40 |
| 5.7  | Demonstration of fiber sliding by using a locking system with the hard rubber layer. . . . .               | 40 |
| 5.8  | Response in terms of strain ( $\epsilon$ ) and wavelength ( $\lambda$ ) for the long line. .               | 41 |
| 5.9  | Comparison between Theoretical and Experimental curves for the long line. . . . .                          | 42 |
| 5.10 | Comparison of the response of the short, intermediate and long line in terms of strain. . . . .            | 43 |
| 5.11 | Repeatability test with locking system with hard rubber. . . . .   | 44 |
| 5.12 | Incremental load step test with locking system with soft rubber on short line $L_o=58.59$ mm. . . . .      | 46 |
| 5.13 | Incremental load step test with locking system with soft rubber on short line $L_o=228.94$ mm. . . . .     | 46 |
| 5.14 | Detail of sliding and deformation in terms of strain for the long line. .                                  | 47 |
| 5.15 | Cavity of the soft rubber. . . . .   | 47 |
| 5.16 | Repeatability test with locking system with soft rubber on long line $L_o=228.94$ mm. . . . .              | 48 |
| 5.17 | Comparison of response by using two different concepts of locking systems. . . . .                         | 50 |
| 5.18 | Response in terms of $\Delta L$ [mm] of locking system with containers. . .                                | 50 |
| 5.19 | Response in terms of $\Delta L$ [mm] of locking system with rectangular plates. . . . .                    | 51 |
| 5.20 | Ten seconds blocks of measurements without all transients. . . . .   | 52 |

|      |   |    |
|------|---|----|
| 5.21 | Comparison between theoretical and experimental (no corrective coefficient) curves. . . . .   | 53 |
| 5.22 | Comparison between theoretical and experimental (with corrective coefficient) curves. . . . . | 53 |
| 5.23 | Comparison between theoretical and experimental (no corrective coefficient) trend. . . . .    | 54 |
| 5.24 | Comparison between theoretical and experimental (with corrective coefficient) curves. . . . . | 54 |
| 5.25 | Comparison between theoretical and experimental curve by increasing load steps. . . . .       | 58 |
| 5.26 | Comparison between theoretical curve and experimental curve with linear fit. . . . .          | 58 |
| 5.27 | Comparison between theoretical curve and experimental curve with correction. . . . .          | 59 |
| 5.28 | Comparison between theoretical curve and experimental curve with correction. . . . .          | 59 |
| 5.29 | Comparison between theoretical and experimental trend by increasing load steps. . . . .       | 61 |
| 5.30 | Comparison between theoretical and experimental trend with linear fit. . . . .                | 61 |
| 5.31 | Comparison between theoretical and experimental trend with correction. . . . .                | 62 |
| 5.32 | Comparison between theoretical and experimental trend with linear fit and correction. . . . . | 62 |
| 5.33 | Repeatability load step Test by starting with pre-load of 0.30 mm. . . . .                    | 64 |
| 5.34 | Repeatability load step Test by starting with pre-load of 0.20 mm. . . . .                    | 64 |
| 5.35 | Repeatability load step Test by starting with pre-load of 0.10 mm. . . . .                    | 65 |

# List of tables

|      |  |    |
|------|--|----|
| 5.1  | Incremental load step test with hard rubber and $L_o=53.59$ mm. . . .                                  | 35 |
| 5.2  | Incremental load step test with hard rubber and $L_o=128.80$ mm. . . .                                 | 38 |
| 5.3  | Incremental load step test with hard rubber and $L_o=228.94$ mm. . . .                                 | 41 |
| 5.4  | Repeatability load step test with hard rubber and $L_o=228.94$ mm. . .                                 | 43 |
| 5.5  | Incremental load step test with soft rubber with $L_o=58.59$ mm and<br>$L_o=228.94$ mm. . . . .        | 45 |
| 5.6  | Repeatability load step Test for comparison of two concepts. . . . .                                   | 49 |
| 5.7  | Incremental load step test for corrective coefficient. . . . .   | 52 |
| 5.8  | Corrective coefficient values for the first type of locking system. . . .                              | 55 |
| 5.9  | Corrective coefficient values for the second type of locking system. . .                               | 55 |
| 5.10 | Incremental load step Test for comparison between two different lines.                                 | 57 |
| 5.11 | Corrective coefficient values for the fiber optic mounted on the short<br>line $L_o=53.59$ mm. . . . . | 57 |
| 5.12 | Incremental load step Test for comparison. . . . .   | 60 |
| 5.13 | Corrective coefficient values for the fiber optic mounted on the long<br>line $L_o=228.94$ mm. . . . . | 60 |
| 5.14 | Repeatability load step Test for the long line $L_o=228.94$ mm. . . . .                                | 63 |



# Chapter 1

## Introduction

Nowadays, the usage of fiber optics is common in several daily applications. In particular, we can find fiber optics in applications such as the telecommunications and sensoristic. In the telecommunications field, the usage of fiber permits to have many advantages compared to the state of art that is the usage of copper cables. In fact, fiber optics allow to transmit big data with high bit rate and for long distance. Therefore, they allow doing this with low losses and there is no need to use an external power supply. In addition to these advantages, the fiber optics are immune to electromagnetic interference and it is possible to use fiber optics in harsh environment thanks to their high temperature resistance and to corrosive environment. As written above, fiber optics can be used also in the sensoristic field and in particular we discuss about Optical Fiber Sensors (OFS). Obviously, they have the same properties and characteristics of fiber optics, so they have the same advantages of fiber optics. Regarding to OFS, there are many types of sensors but we have focused on *Fiber Bragg Gratings* (FBG) and they represent the object of study of this work. These types of sensors can be used in several daily applications of fields of medicine and engineering from Civil to Aerospace engineering. In particular, in Mechanical and Aerospace engineering they are used to measure strain, temperature, pressure, vibration and others important physical quantities. These quantities are computed by using appropriate equations that relate wavelength variations detected by FBG and these physical quantities. Hence, with the FBG sensors it is possible to monitor structure health and allow the mechanical and thermal diagnostics and prognostics.

## 1.1 Objectives

The aims of this work are to study and test FBG sensors and to design different types of locking systems that allow to lock the fiber optic to the structure that we want to monitor. In order to accomplish these objectives, the work has been divided in four fundamental steps:

1. To design and manufacture locking systems to lock the fiber optics.
2. To assembly a test bench.
3. To perform measuring campaigns to test the FBG sensors and to test the performances of locking systems.
4. To choose the optimal locking system and to show the most important results obtained.

## 1.2 Thesis structure

This Thesis is structured into six chapters that are *Introduction*, *Fiber Optic and Optical Fiber Sensors*, *Assembly of Test bench*, *Matlab script for the Post-processing, Tests and Measurements* and *Conclusions*.

The chapter *Fiber Optic and Optical Fiber Sensors* presents the main physical principles in which the mode of operation of fiber optic is based, an overview of materials for the manufacturing of fiber optics. Also advantages and disadvantages are listed showing a brief comparison between fibers and electric cables. Then, the chapter presents a brief overview about the Optical Fiber Sensors and in particular about the FBGs, showing the fundamental equations and the principle of operation.

The chapter *Assembly of Test bench* shows whole assembly phase of test bench. In particular, there was the need to block the fiber to perform mechanical and thermal tests and for that reason it was necessary to design and manufacture different types of locking systems. In particular, the designed locking systems differ each other according to the type of test to do. It will show CAD models and final products. Therefore, all components that constitute the test bench and all adopted adjustments are shown and explained, respectively. The adjustments adopted are about the design of locking systems and to make the measurements more accurate.

The chapter *Matlab script for the Post-processing* presents an overview about the Matlab script used for the post-processing of raw data obtained by the *Interrogator*.

The chapter *Tests and Measurements* shows the main and significant results obtained during the measurement campaigns. Different type of tests have been done varying the locking system and the initial length  $L_o$  of each line arranged on the breadboard.

The chapter *Conclusions and Future works* shows the optimal configuration obtained that guarantees the best results in terms of strain variations or displacement  $\Delta L$  [mm]. Moreover, there is a list, for other people who will work to this research project in the future, of advices about the other type of tests to perform.

# Chapter 2

## Fiber Optic and Optical Fiber Sensors

Nowadays, the fiber optic is becoming more and more employed in most of daily applications such the telecommunications. Moreover, there is the possibility to use the fiber optic as a sensor, especially in fields of engineering such as Civil, Mechanical and Aerospace engineering. The peculiarity of the fiber optics is the carriage of the light inside the fiber core with the minimum signal attenuation and, regarding to this, the final achieved value of the lowest loss is only  $0.2 \text{ dBkm}^{-1}$  [1]. In addition to this, the fiber optics are immune to EMI (Electromagnetic Interference) [2]. However, an overview of advantages and disadvantages of fiber optics are explained in detail in the paragraph *Advantages and Disadvantages of using the Fiber Optic*.

### 2.1 Overview of Materials

The most of common fiber optics are made of glass or plastic material. The choice of the material is given by the purpose of the application. In fact, the plastic optical fibers (POF), having high attenuation, are used for short-distance applications and with low-bit-rate transmission systems [3]. Therefore, POF are cheaper and more flexible than glass fibers [3]. Glass fibers have a low transmission optical loss, so they are used for long distance applications and when it has a high bit rate of transmission. Glass can be doped to increase or reduce the refractive index. Usually, to increase refractive index are used something like Germanium dioxide  $\text{GeO}_2$ , Phosphorus pentoxide  $\text{P}_2\text{O}_5$ , Titanium dioxide  $\text{TiO}_2$  and Aluminium oxide  $\text{Al}_2\text{O}_3$ , on the other hand to reduce refractive index Boron trioxide  $\text{B}_2\text{O}_3$  and Fluorine  $\text{F}$  can be used [4]. For example,  $\text{GeO}_2$  and  $\text{P}_2\text{O}_5$  have the peculiarity to increase the refractive index so they are suitable for fiber core [5], on the other hand dopants

such as  $F$  and  $B_2O_3$  are suitable for cladding because they decrease the refractive index [5].

## 2.2 Geometry and basic classification of Fiber Optics

In general, the fiber optic has a cylindrical geometry and it is constituted by a core, a cladding and an external coating, see the following figure 2.1.

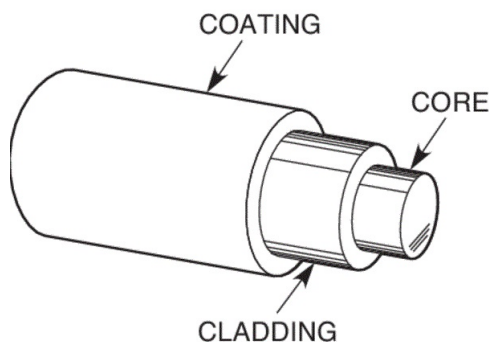


Figure 2.1. Example of fiber optic structure. (©2018 Newport Corporation. All rights reserved)

A classification of the fiber optic based on the modes of light propagation is:

- *Single-mode fiber optic.*
- *Multi-mode fiber optic.*

The Single-mode fiber optic (SI) supports only one propagation mode and has a core thinner than the Multi-mode fibers (MM) core, see 2.2 (figure from [6]). In fact, the second one has a core diameter of about  $50 \mu m$  (or more), instead the single mode fibers have a core diameter of about  $10 \mu m$ . The dimension of the cladding is  $125 \mu m$  and this value is standardised for all type of fiber optics except in some cases.

Thanks to the large Numerical aperture (see equation 2.7) of a multi-mode fiber, more light can be sent inside the fiber by using an inexpensive optical source such a LED [3]. Therefore, having a large core, this fiber class is easier to splice than single-mode fibers. On the other hand, multi-mode fiber optics have some disadvantages. In fact, due to intermodal dispersion, they are not suitable for long-haul and/or in applications with a high-bit-rate[3]. For this reason, for applications with long-haul and/or high-bit-rate, single-mode fiber optic are suitable because they permits

applications with haul from 1000 km to 30000 km and with a high-bit-rate from 10 Gb/s to 100 Gb/s [3].

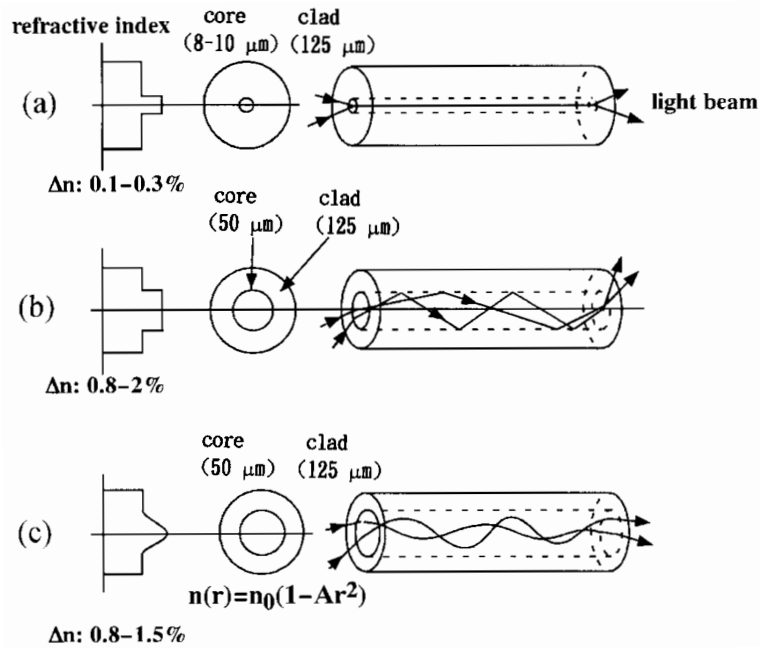


Figure 2.2. (a) Single-mode fiber, (b) Multi-mode fiber of step index type, (c) Multi-mode fiber of graded index type. [6]

Another classification of the fiber optics is based on the refractive index of core:

- *Step index fiber optic.*
- *Graded index fiber optic.*

In the first type of fiber class, calling  $r_1$  radius core and  $r_2$  radius cladding, there are various diameter ratios: 8/125, 50/125, 62.5/125, 85/125 and 100/140 [ $\mu\text{m}/\mu\text{m}$ ] [7]. In this class of fiber, the refractive index of core and cladding are constant and uniform. But, the refractive index drastically changes to core-cladding interface and  $n_1$  and  $n_2$  are slight different. In particular,  $n_1$  is the refractive index of the fiber core and  $n_2$  is the refractive index of the fiber cladding. This slight difference between the value of those two refractive index, is obtained by adding a low concentrations of dopants [7].

In the graded index fibers, the refractive index of the cladding is constant and uniform but the refractive index of the core changes gradually, nearly parabolic, with a maximum value along the axis of fiber until the minimum value along the core-cladding interface. Hence, the refractive index of the core is a function of  $r$ , where  $r$  is the radial position. Materials for Graded index fibers, are obtained by adding dopants in correct concentrations [7], and because of this particular variation

of refractive index the optical ray does not follow a straight line along the fiber but a curved line [7]. The general function that describes the refractive index variation of graded index fibers, it is the following relation 2.1 taken from [7]:

$$n^2(r) = n_1^2 \left[ 1 - 2 \left( \frac{r}{a} \right)^p \Delta \right] \quad r \leq a \quad (2.1)$$

Where  $p$  is called *grade profile parameter* and varying his value from 1 to  $\infty$ , it is possible to obtain different refractive profile, and  $\Delta$  is the *normalized refractive index*.

## 2.3 Physical Principles behind Fiber Optics

The propagation of light into the fiber core is based on the Total Internal Reflection (TIR). Thanks to this, the light is confined into the fiber core. This phenomenon takes place when the refractive index of the core is higher than refractive index of the cladding. Moreover, the incidence angle has to be higher than the Critical Angle and this angle is computed with equation (2.4). Instead, regarding to the refractive index is computed with the following equation (2.2):

$$n = \frac{c}{v} \quad (2.2)$$

Where:

- $n$ =refractive index of medium.
- $v$ =speed of light (in medium).
- $c$ =speed of light (in vacuum).

In accordance with the optical phenomenon described above, it is necessary to introduce the fundamental Snell's Law (2.3):

$$n_1 \cdot \sin\alpha_i = n_2 \cdot \sin\alpha_r \quad (2.3)$$

Where:

- $n_1$ =refractive index of the first medium.
- $n_2$ =refractive index of the second medium.
- $\alpha_i$ =incidence angle.

- $\alpha_r$ =refractive angle.

The Critical (or Limit) angle is defined by the following equation (2.4):

$$\theta_c = \arcsin \frac{n_2}{n_1} \quad (2.4)$$

This angle is obtained when the refractive angle  $\alpha_r$  is  $90^\circ$ . Beyond this angle, the light is totally reflected. Moreover, it is necessary that light rays are sent inside the core with an angle minor the  $\alpha_{max}$ , so that the light can propagate along the fiber, see 2.3 (figure from [8]):

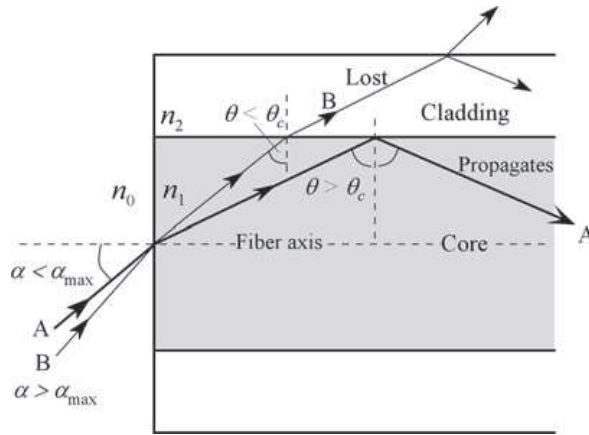


Figure 2.3. Main angles of a fiber optic. [8]

The  $\alpha_{max}$  above written and indicated in figure 2.3 is the *maximum acceptance angle* [8]. This angle defines the range in which light can be sent inside the core for TIR takes place, instead beyond the highest acceptance angle, total reflection does not exist. It is possible to obtain  $\alpha_{max}$  with the following steps. To the interface between the core and external medium (generally the air), we can write:

$$n_0 \cdot \sin(\alpha) = n_1 \cdot \sin\left(\frac{\pi}{2} - \theta_c\right) \quad (2.5)$$

Moreover:

$$n_1 \cdot \sin(\theta_c) = n_2 \cdot \sin\left(\frac{\pi}{2}\right) \quad (2.6)$$

We get:

$$\sin(\alpha_{max}) = \frac{(n_1^2 - n_2^2)^{1/2}}{n_0} \quad (2.7)$$

Where:

- $n_1$ =refractive index of the core.
- $n_2$ =refractive index of the cladding.
- $n_0$ =refractive index of the external medium (in general is air).

The numerator of equation 2.7 represents the NA (*Numerical Aperture*):

$$NA = (n_1^2 - n_2^2)^{1/2} \quad (2.8)$$

## 2.4 Advantages and Disadvantages of using the Fiber Optic

The most important advantages of the fiber optics are:

- The first advantage of fiber optic is a low attenuation of the signal. Especially, in communication systems, it represents an important advantage because it permits to transmit the signal over a long distance. On the other hand, a common copper wire does not allow it.
- The fiber optics are transparent to the electromagnetic radiations and immune to lightning due to the glass that is a good dielectric, as written in [4]. This advantages is important especially in Aerospace and Space applications where there is a large number of, for example, electronic devices.
- In the case of glass fiber optics, due to the high fusion temperature of the glass, the fibers are resistant to high temperatures.
- The fiber optics, in general, are made of glass materials. This kind of materials are stable chemically, free from rust and resistant to corrosion, instead of the metal materials. [4]. For this reason, fiber optics can be used in harsh environment. Therefore, they can be used in environments which can catch fire or flammable, because of they do not creat sparks [4].
- The material used is glass (silica) that is very abundant on the Earth instead of copper [4].

- The fiber optics are lighter and smaller. Consequently, it permits to install fiber optics easily inside a structure because of the reduction of the bulk. Considering a plastic coated fiber, the outer diameter is around 1 mm in respect of communication cable that has an outer diameter of 1 to 10 mm [4]. This advantage also permits to abide by a particular weight constrain.
- The fiber optics are broadband and it allows sending and receiving a lot of information in high transmission speed.
- The fiber optics is not expensive.

Main disadvantages of fiber optics are:

- The utilisation and maintenance of fiber optic are not cheap because they need to use many equipment that are so expansive. For example, for the utilisation of FBG sensors it is necessary an expensive interrogation system or also expansive equipment are required to splice two or more fiber optics.
- The fiber optics have to be installed without high curve radius because of the increase optical losses.
- During the installation, the fiber optic is susceptible to damage because the fiber is thin and susceptible to mechanical damage.

## 2.5 Fiber Bragg Grating Sensors

Sensors, regardless of their field of application, represent a very important elements within a system. For example, in the case you have the equipment automatically controlled, the sensors are important to have feedback signals, in engineering applications such as in the case of Civil and Aerospace Engineering, the sensors are very important to monitor the structures by measuring for example strain, stress and temperatures variations, up to the medical field in which an Optical Fiber Sensor (OFS) may be able to transmit biochemical information [9].

The optical fiber sensors represent a new frontier in sensor technology. In dependence on physical quantities detected, OFS can be divided in different classes such as *geometrical, mechanical, dynamical, physical, chemical and biochemical, miscellaneous* [9].

In particular, we discuss about the *Fiber Bragg Grating* (FBG) sensors. The development of this new technology has slowed because of high cost, but during the

years due to the development and production on a more wide-scale, optical fiber sensors are getting more used in several fields of engineering. In the Aerospace and Mechanical field, the FBGs are employed to measure physical quantities such as:

- Strain.
- Vibration.
- Temperature.
- Pressure.

One of the most important advantage of this kind of sensors, it is its immunity to electromagnetic radiation and interference. In addition to this advantage, this new technology does not need of external electric power source and electric cables. However, because FBGs are written in fiber core, they have all advantages that are typical of fiber optics such as to be immune to EMI, electric isolation, to be immune in harsh environment with high temperature and corrosive elements, low loss even with long distance, to be light and small and to be multiplexed. It is possible to inscribe dozens of FBG sensors in a single fiber optic and, in addition to this, each inscribed sensor can detect a particular physical quantity.

On the other hand, there are some disadvantages to use optical fiber sensors and either these are the same for fiber optics. In fact, fiber cables with optical sensors are not easy to install, because fiber optics are very susceptible to mechanical damage and to different kind of losses that are typical of fiber optic itself such as, for example, losses that depend on bending or curvature of fiber. During the assembly of test bench and during the testing phase, these disadvantages are taken account into lock fiber optics to the locking systems.

Regarding to the multiplexing, as above written, represents a great advantage because in a given fiber optic it is possible to write a certain number of FBGs with different  $\lambda_B$ . On the other hand, there are some aspects to consider. In fact, the fiber optic is constituted by a core, a cladding and an external coating and to insert one more FBG sensor in fiber optic, the external coating has to be removed and a splicing process has to be performed. This process permits us to join two or more fiber optics with different FBG sensors. But, after having remove the external coating, it is important to recoat the fiber. Two methods may be such as the use of a machine for the recoating or the use of a heat shrinkable tube. The first method permits to obtain almost the same performance of original fiber optic, but it is expensive and it needs of particular facilities. The second method, on the other hand,

is easy and it needs only a heat source. Obviously, this method does not guarantee the same performance of the original fiber optic. Another solution to obtain a fiber optic with several optical sensors, it is to use just one fiber optic and to write on it the desired number of FBG sensors by avoiding the disadvantages above written about the splicing method.

### 2.5.1 Fundamental equations of FBGs

The first fundamental equation of fiber Bragg grating is the following relation:

$$\lambda_B = 2n_{eff}\Lambda \quad (2.9)$$

Where:

- $\lambda_B$ =Bragg wavelength.
- $n_{eff}$ =effective index of the grating.
- $\Lambda$ =Grating period.

The grating represents a section of fiber optic where the refractive index of the core is modulated periodically [9].

In case of mechanical or thermal tests, a shift of this wavelength occurs. In particular, the equation that considers the contribute of strain and temperature variations is the following equation [10]:

$$\Delta\lambda_B = \lambda_B[(\alpha_f + \zeta_f)\Delta T + (1 - P_e)\epsilon] \quad (2.10)$$

Where:

- $\lambda_B$ =Bragg wavelength.
- $\alpha_f$ =Thermal expansion coefficient of fiber optic.
- $\zeta_f$ =Thermo-optic coefficient.
- $P_e$ =Photoelasticity constant.
- $\Delta T$ =Temperature variation.
- $\epsilon$ =Strain.

An illustrative figure about the fiber Bragg grating is shown in figure 2.4 [8].

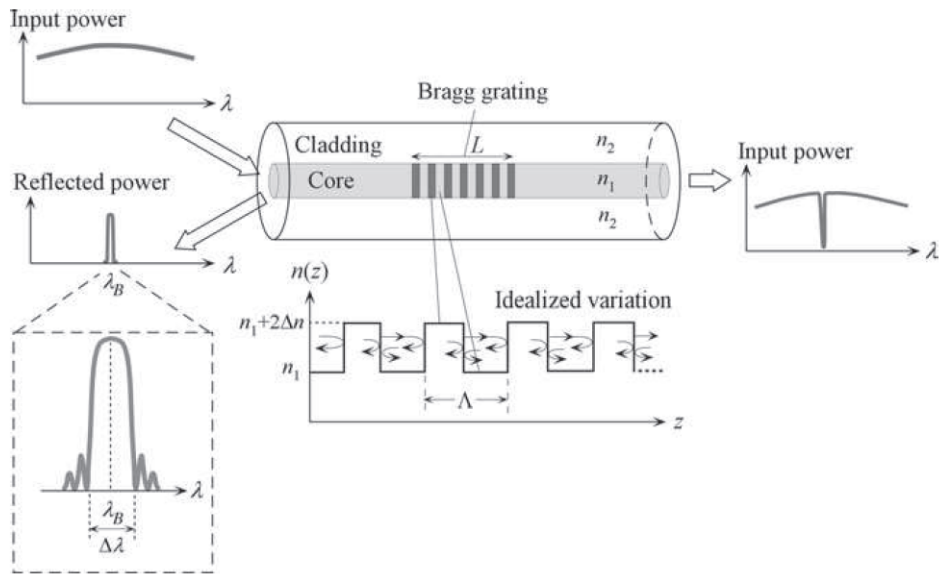


Figure 2.4. Summary of the main characteristics of the Fiber Bragg Grating sensors [8].

By applying a load, for example, a shift of the wavelength occurs, as shown in the following figure 2.5, because of the variations of the properties of the grating.

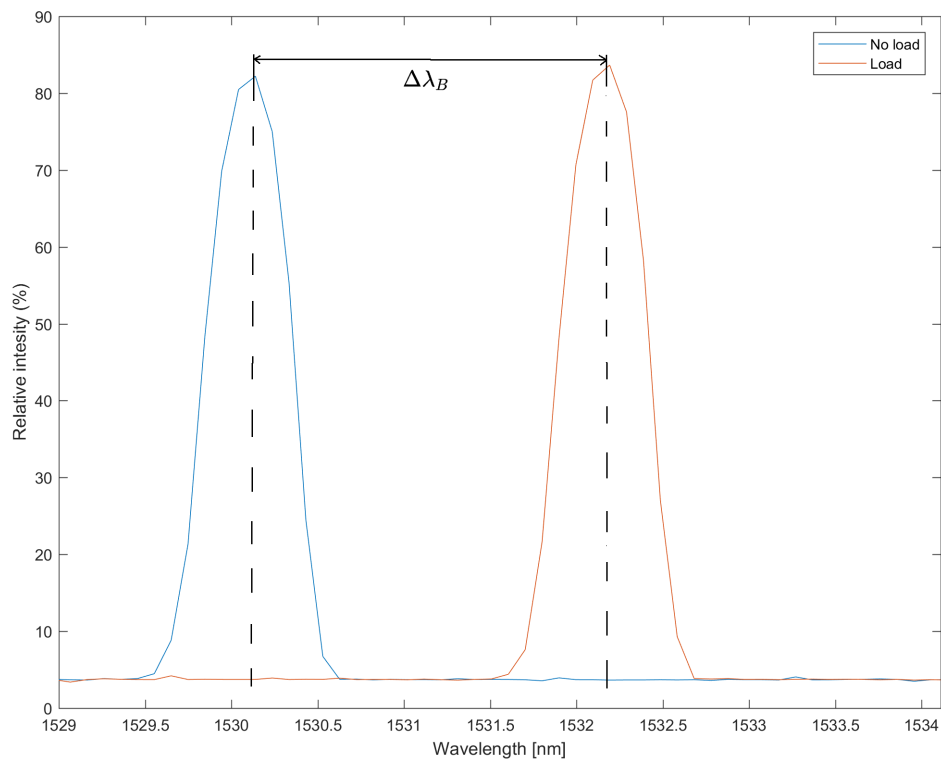


Figure 2.5. Shift of the wavelength due to an application of a load.

This is a typical behaviour observed during our measurement campaigns.

# Chapter 3

## Assembly of Test Bench

In this chapter, the assembly phase of test bench is explained. The test bench is fundamental to study the FBG sensors and the quality and the performances of the locking systems designed by us to lock the fiber optics. In particular, different types of the locking systems were designed, by making CAD models with the software *SolidWorks*, to perform mechanical and thermal tests. Therefore, the CAD models and final manufactured locking systems are shown in this chapter. Moreover, all the adjustments taken during the design process of these systems and during the assembly of bench are explained.

### 3.1 Platform

The facility constituted by locking systems, micro translation stages and fiber optics, are mounted on two different breadboards and each of them is used for mechanical and thermal testing, respectively. In the beginning of testing phase, the breadboard was mounted on a wood platform, but measurements were strongly susceptible to vibrations. In fact, each FBG has a particular *Center Wavelength* called *Bragg Wavelength*  $\lambda_B$  and this wavelength shifts in response to strain or temperature variations, so vibration causes an additional shift of  $\lambda_B$  reducing the accuracy of measurements. Therefore, this external noise does not to permit us to choose a reference wavelength to start a given test. Due to this, anti-vibrational facilities have been chosen for testing phase. In fact, the breadboards are located on anti-vibration platform and, in particular, for the breadboard dedicated to mechanical tests passive dumpers have been used (see figure 3.1) to achieve an additional vibration isolation. In particular, the breadboard for mechanical testing is enclosed in a box (optical enclosure) made by Plexiglass panels, see figure 3.2. By using this box, we reduce the negative effects caused by vibration caused by *wind* and *sounds*. Instead, the

breadboard for thermal testing is not enclosed because of, as shown below, fiber optic is locked inside a closed package that is not susceptible to vibrations caused by sound or wind.

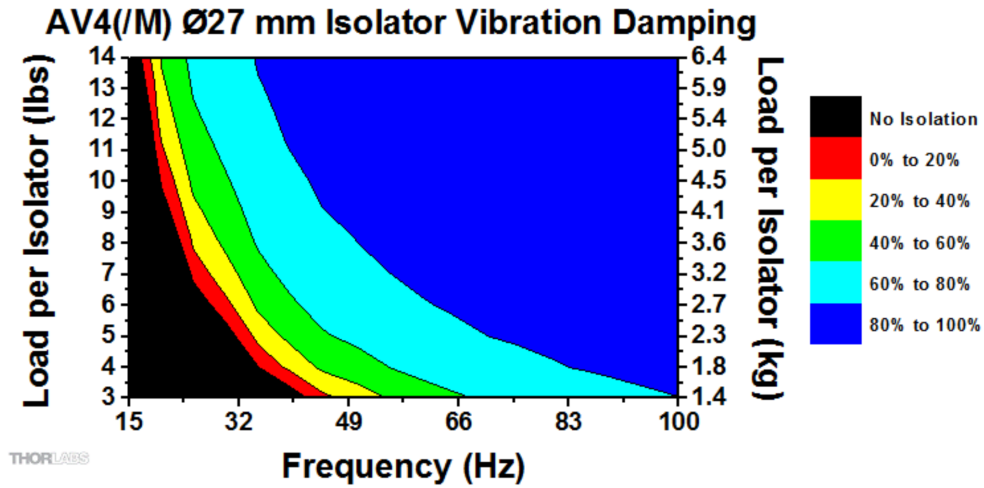


Figure 3.1. Load-Frequency per each passive dumper (*Copyright 1999-2018 Thorlabs, Inc.*).

In particular, the posterior Plexiglass panel was customized, i.e. four holes were done to permit the inserting of optical fibers to connect to the *interrogator*.



Figure 3.2. Optical enclosure (*Copyright 1999-2018 Thorlabs, Inc.*).

## 3.2 Locking Systems for Mechanical tests

### 3.2.1 Aluminium Locking Systems

Different types of locking systems are designed to perform mechanical tests. The first type of locking system for mechanical testing is based on three components that are two aluminium components (upper and bottom base) and a rubber layer, see figure 3.3. This type of locking system is designed with the aim to lock both ends of optical fiber and to permit the usage of different materials to insert between the two aluminium bases and the fiber. Therefore, this system permits the interchangeability of fiber optics and by locking both ends of fiber optic, it is possible to apply a load in terms of strain ( $[\mu\epsilon]$ ) variations or  $\Delta L$  ([mm]) on the fiber by using a micro translation stage.

It is fundamental to insert a medium between fiber and the aluminium locking components, because of the fiber crushing. In this regard, two tests were performed, in which in the former no rubber layer has been located between two aluminium components and the fiber, in the latter a double-sided tape has been used, inserting a piece of tape on each aluminium base. In both tests, the fiber crushing has happened. Hence, it is advisable to use always an intermedium layer that avoid the damage of the optical fiber.

At first, in order to avoid this crushing, it was decided to insert a rubber layer. In the beginning, a *hard* rubber layer has been used such medium, then a *soft* rubber has been used. The choice about which kind of rubber to use is a critical point; in fact, this choice influences the measurements severely because of the deformation of the rubber, and besides, the fiber could slides between the aluminium bases and the rubber layer itself.

The first package is shown in figure 3.3 and from the top to the bottom are shown the upper base, the rubber layer and the bottom base. The size of the bottom component is chosen in compliance with the size of micro translation stage, because this bottom base is mounted on it. In particular, the driver that causes the deformation of fiber optic is a *X axis Aluminum translation stage*.

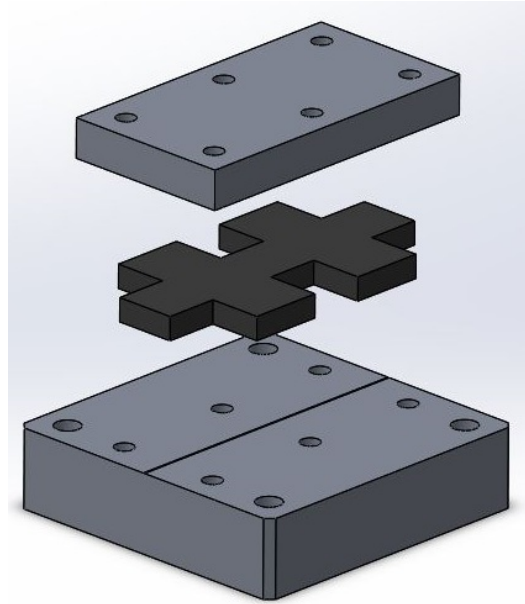


Figure 3.3. Package of locking system for mechanical tests.

On the upper base there are six holes to permit the inserting of six screws and to permit an uniform distribution of pressing load. Due to this adjustment, we achieve a correct locking of the fiber.

Regarding to the shape of rubber shown in figure 3.3, it is only an approximate shape, because you may choose to insert a rubber layer with different shape such a rectangular shape.

Instead, the second locking system is directly mounted on the breadboard. This is constituted by an upper base that is the same to the upper base shown above, a bottom base (see figure 3.4) and a rubber layer that is inserted between these aluminium bases.

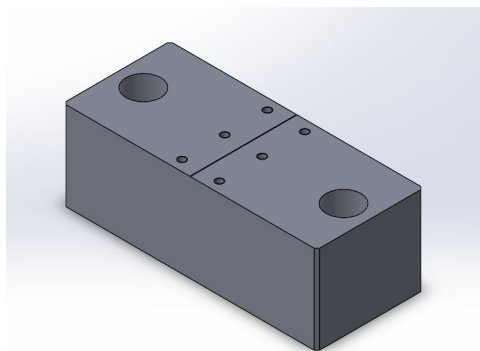


Figure 3.4. Bottom base mounted on breadboard.

These types of locking systems are based on mechanical locking of fiber optic

and they are designed to have a system that permits to lock the fiber without the use of glue. Therefore, they represent a good solution that permit to substitute fiber optic easliy and quickly.

The final packages are shown in the figures below 3.5 and 3.6:

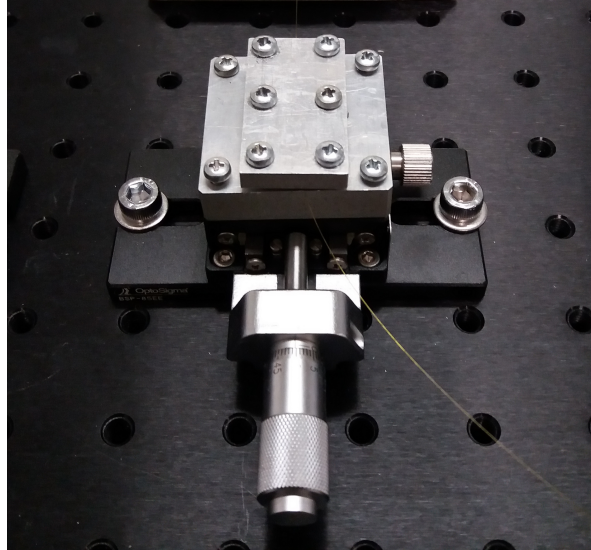


Figure 3.5. Package located on the micro translation stage.

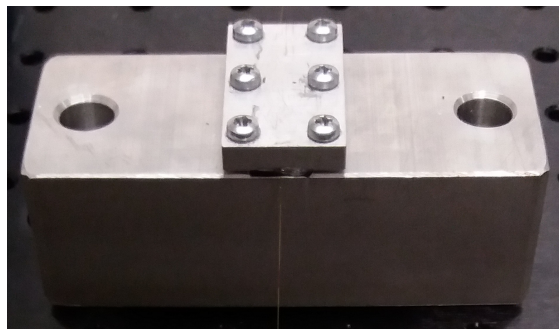


Figure 3.6. Package located directly on the breadboard.

You can see in figure 3.5 that micro translation stage is mounted on the breadboard by using an adaptor, because of the mounting holes of micro translation stage are not suitable with holes of the breadboard.

Regarding to the bottom bases, it should be noted that on each of them, a v-groove of about 1/10 mm in depth has been made to host a part of fiber optic. The horizontal center line visible on the figure below is the *v-groove*, see figure 3.7. It is fundamental do not make a groove deeper, because the fiber would be completely located inside the groove not allowing the correct lock of itself and it would not be possible to apply a load on fiber. Therefore, this groove permits to align the fiber accurately.



Figure 3.7. V-groove.

Once designed and manufactured the locking systems, these are mounted on the breadboard by setting four different *lines*, see figure 3.8.

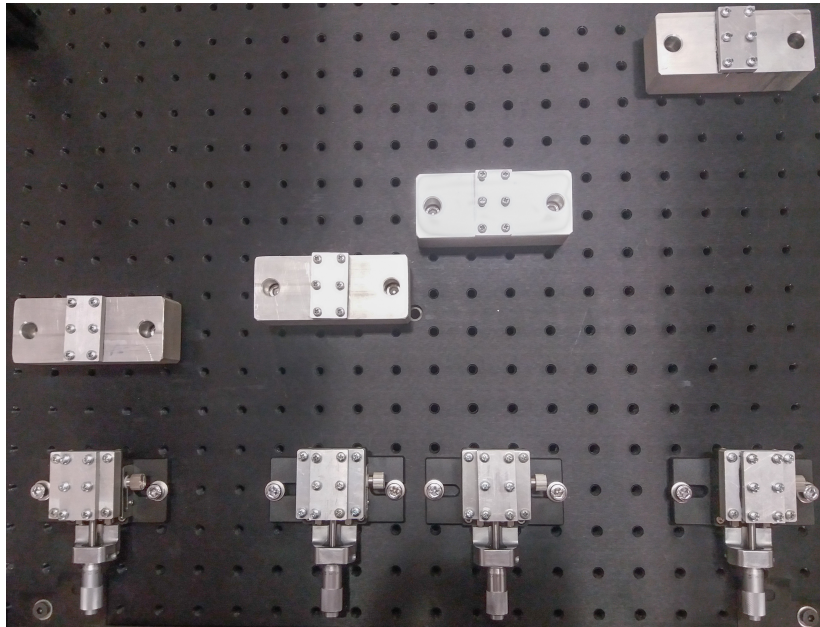


Figure 3.8. Set-up for Mechanical tests.

These different configurations permit us to study the response of the FBG sensors in terms of strain variations applied by the micro translation stage. Therefore, the strain values change based on the  $L_0$  that is the initial length of the fiber optic on each line. However, in the chapter *Tests and Measurements* are shown the important results obtained varying  $L_o$ .

There are two adjustments to adopt during the mounting of locking systems and fiber optics; first of all, it is important to prepare the upper aluminium component accurately. In fact, a piece of rubber is glued on this component and when you screw that on bottom base, rubber layer flattens (see figure 3.9) causing the cut of fiber

optic. For this reason, it is important to cut accurately, in terms of length, the piece of rubber to be sure when you screw the upper component that this action does not cause the cut of fiber optic. The second adjustment is about fiber optic, namely it is necessary to use a pair of gloves to touch the fiber ends, because the body humidity and dust can encourage the fiber sliding on rubber-aluminium interface.



Figure 3.9. Flattening of the rubber layer.

### 3.2.2 3D Printed Locking Systems

In addition to the aluminium locking system, two different concepts of locking system have been designed and manufactured by using the *3D Printing*. These new systems are used in order to lock the fiber optic by using resin, avoiding to damage of aluminium components shown above. It was decided to use the 3D printing technology because it enable us to obtain necessary components in the brief time and with low-cost. Therefore, this technology permits to manufacture mechanical parts, for example, with high complexity shape without increasing of cost and time.

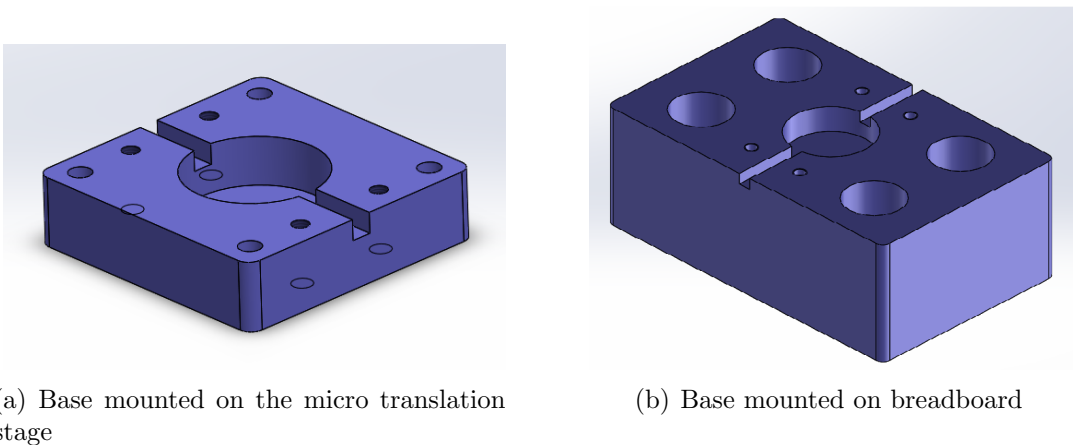


Figure 3.10. Locking system in Polylactic Acid (PLA).

The first concept consists of two locking systems of which the first one is located on the micro translation stage and the second one is mounted directly on the breadboard. The central circular hole is the location for a container where we cast the resin permitting to lock the fiber inside it. Therefore, in the figure 3.11, you can see two cuts for hosting the fiber and this system permits to the resin to cover the fiber completely. To avoid that containers escape from their hosting circular hole, rectangular plates have to be putted on the two bases shown above.

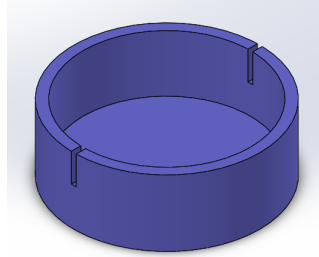
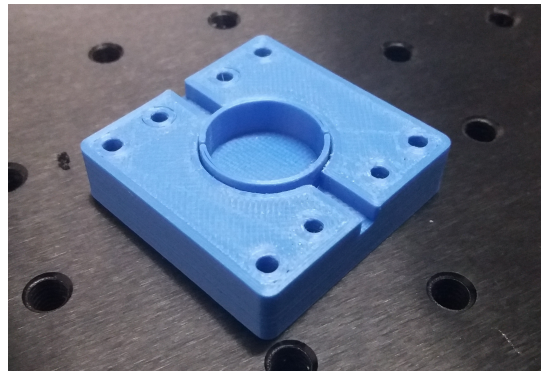
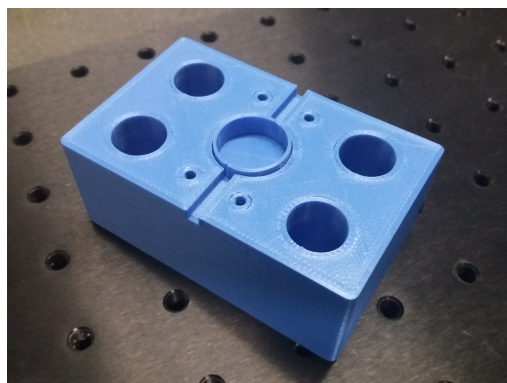


Figure 3.11. Container for resin.

The final manufactured products are shown in figures 3.12 and 3.13:



(a) Base on micro translation stage



(b) Base on breadboard

Figure 3.12. Final manufactured products.



Figure 3.13. Container for resin.

If the fiber breaks during a strain test or if you need to use another fiber optic, this locking system permits us to substitute the container easily and quickly.

Regarding to the second concept, it is based on two rectangular plates. Both ends of fiber optic is glued on these plates 3.14:

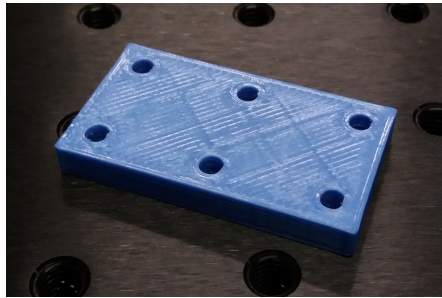


Figure 3.14. Rectangular plate.

In this case, if the fiber breaks you should try to remove mechanically the resin glued on the plates, but this operation could cause the damage of the components. On the other hand, new rectangular plates have to be printed. Therefore, this concept does not permit the interchangeability of fiber optics, so if you need to use a new fiber, it is necessary to print other rectangular plates. Obviously to print this plate needs a greater quantity of PLA material than the material to print the containers.

An example of final set-up of these two concepts is shown in figure 3.15. On the breadboard, the locking systems are mounted with different value of  $L_o$  for each line. In this way, it is possible to study how measurements change in response to strain applied by micro translation stage and to study how the strain values change in respect of the initial length  $L_o$ . Moreover, two lines are mounted with the same  $L_o$  but with two different concept of locking system. This kind of measure permits us to study the quality of those concepts fixed  $L_o$ .

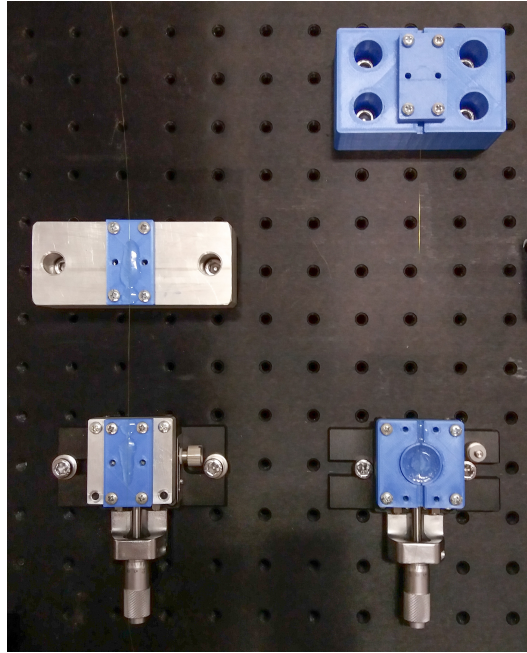
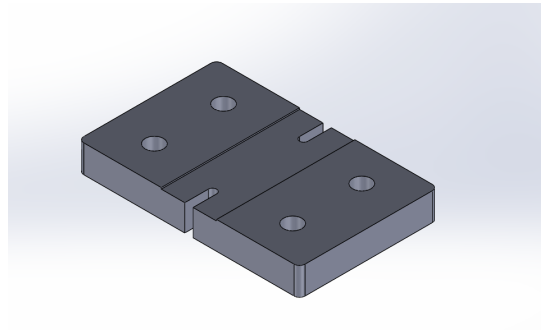


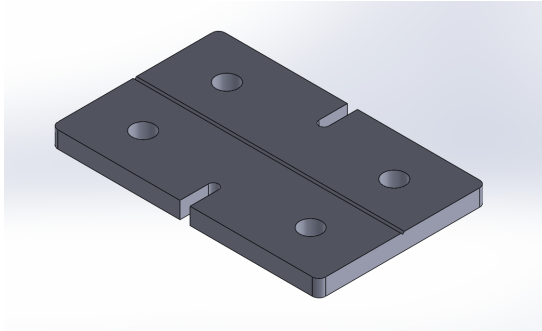
Figure 3.15. Set up of Locking systems for resin.

### 3.3 Locking Systems for Thermal tests

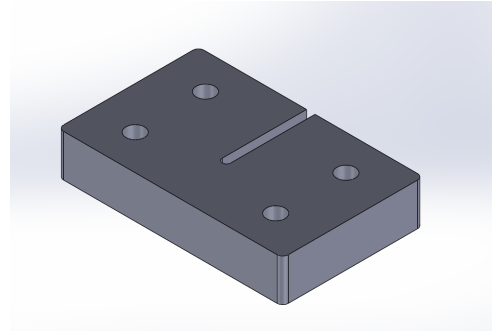
For thermal tests, it has designed and manufactured two concepts. Both concepts are a package of three aluminium components in which the first is a base to host Peltier module, the second is a component to locate fiber optic and the third is a component to insert temperature sensor. On the base for the fiber optic, a v-groove of about 1/10 mm in depth is made to accommodate the fiber in the own base. Instead, regarding to the depth of groove for Peltier module, it have not to be too deep in height because the cold and hot sides of the thermal module have to touch two aluminium components. This package is bolted using four threaded bars and four nuts, and it is mounted on the breadboard used for thermal tests. An adjustment is the use of some spacers between the base for Peltier module and base where is located the fiber; in fact the spacers permit the correct operation of Peltier module because the hot aluminium base is separated from the cold one. In addition to this, the spacers avoid the crushing of the thermal modules.



(a) Base for Peltier module



(b) Base for fiber optic



(c) Base for temperature sensor

Figure 3.16. Three components of the package for thermal tests.

The second concept is quite similar to the first one. The only difference is the design of the base for Peltier module shown in figure 3.17. The central threaded hole ( $M20$ ) is to bolt a bar and the Peltier module is located on the end of the threaded bar. This facility permits to approach the thermal module slowly until it touches the upper base where is located the fiber. Therefore, this system avoids the thermal module crushing, but either way, the spacers are important for the proper operation of the module.

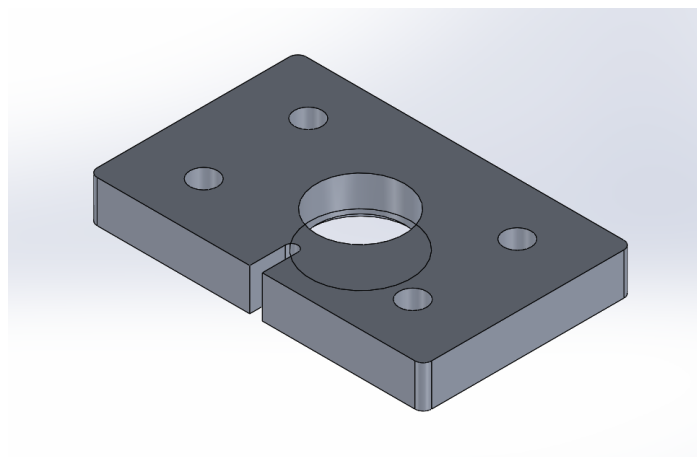


Figure 3.17. Base for Peltier module.

The final package manufactured is:



Figure 3.18. Final package locking system for thermal testing.

Such material for these packages has been chosen the aluminium and all components are made of aluminium to avoid having different coefficients of thermal expansion complicating computes. Regarding to the use of four threaded bars and nuts, this systems permit us to lock the package and to regulate it in heigth. In future tests, this adjustment is important, in particular when there is the necessity to heat and strech fiber optics at the same time.

### 3.4 Splicing of Fiber Optics

During the testing phase, it has been fundamental to splice the fiber optics, because fiber optics with the Bragg grating at our disposal do not have the patchcord for attaching the fiber to the interrogation facility. Nowadays, there are two different methods for splicing fiber optics based mainly on mechanical and fusion splicing, respectively. The kind of splicing chosen by us, it is the fusion splicing. Even if the fusion splicing requires of some expensive equipment, it represents a technique that permits to obtain a high accuracy level with low losses.

At first, it is necessary to remove the external coating with a few adjustments. In our case, the external coating of fiber optic, where there is the patchcord, has been removed mechanically by using a stripper, instead the coating of the fiber optics, where there is the Bragg grating, has been removed by using a heat source and chemistry agent such isopropyl alcohol, because they have a coating made in Polyimide. Once that external coating is removed, it is necessary to clean the ends of each fiber with a solvent, then the fibers have to be cutted with a manual or automatic *cleaver* shown in figure 3.19. The cleaving process is critical, because if the ends of each fiber are not perpendicular to the longitudinal fiber axis, the optical loss estimated increase.



(a) Manual cleaver



(b) Automatic cleaver

Figure 3.19. Two different types of cleavers.

Accomplished the cleaning and cutting, a heat shrinkable tube have to be inserted in one of two fibers. Then, the two fiber optics have to be located inside the *splicer* correctly in proximity to the electrodes, see figure 3.20.

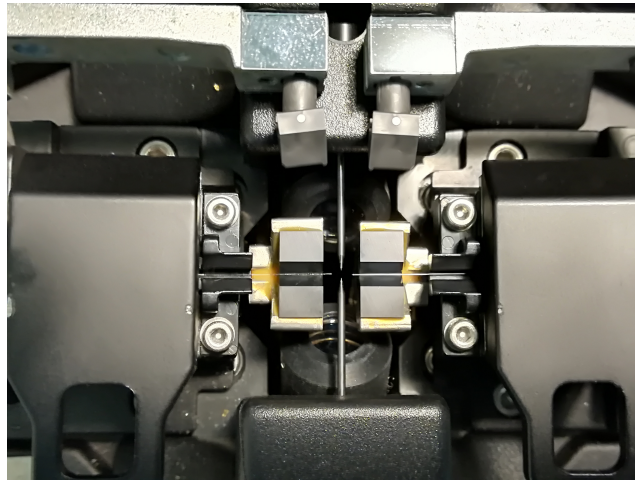
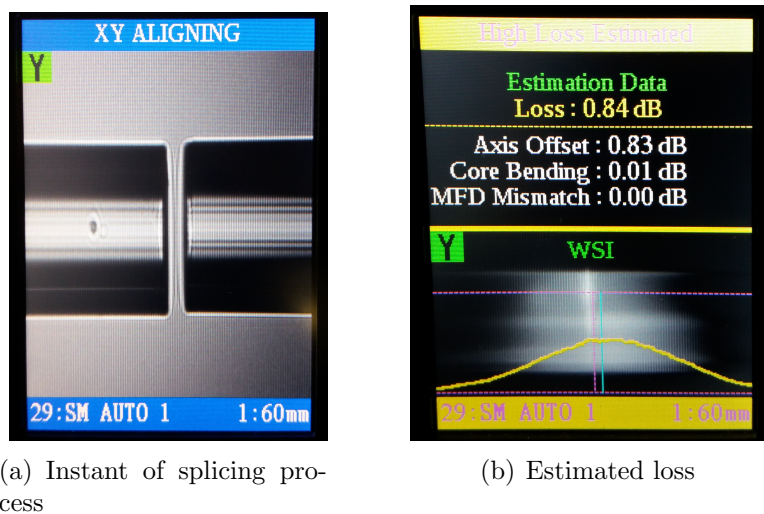


Figure 3.20. Position of fiber optics inside the splicer.

During the splicing process you can see the status of fiber optics and the entire process on the machine monitor, see figure 3.21. In general, if the cut has been correctly the splicing starts. At the end of this process, an estimated splicing loss is displayed on the monitor.



(a) Instant of splicing process

(b) Estimated loss

Figure 3.21. Splicing process and estimated loss shown on the monitor.

Then, you move the heat shrinkable tube shown in figure 3.22 on the joint and put the fiber optic in the heater. The shrinkable tube is important to protect the joint of the fiber optic, in fact the external coating of the fiber ends has been removed before the splicing, for this reason the fiber optic is unprotected after the process.

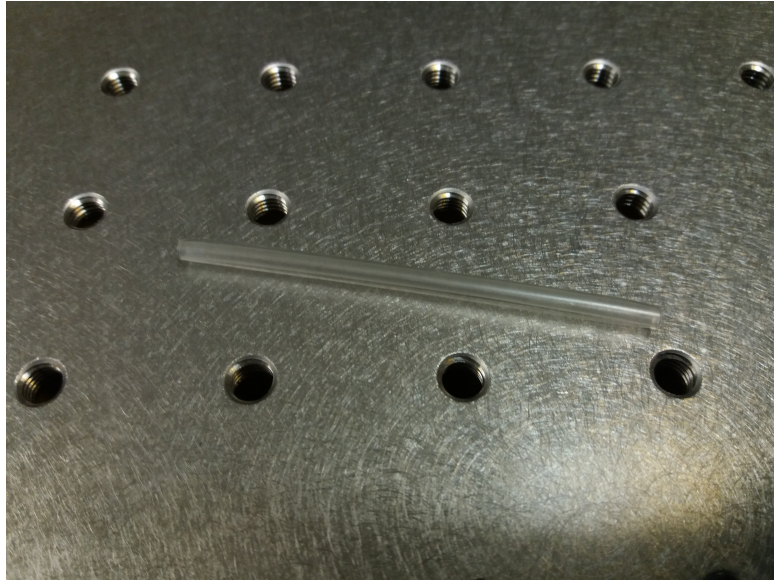


Figure 3.22. Heat shrinkable tube.

### 3.5 Interrogation layout

In addition to the objects explained previously, to achieve the interrogation of FBG sensors, an *Interrogator* has been used. This facility permits us to send a laser beam inside the fiber optic and to interrogate the FBG sensors. Each FBG has a particular *Center Wavelength* called *Bragg Wavelength*  $\lambda_B$  that shifts in response to strain or temperature variations; at the end of a strain test, thanks to the Interrogator, we obtain a *.log* file that has the time steps and all wavelengths detected during a given test. Moreover, the *.log* file can show other features such as strain and temperature directly measured by the Interrogator, and you decide to show those values in the output file by setting the acquisition software of the interrogator. However, it is recommended to process the raw information that is the detected wavelength, and strain or temperature values are obtained by a script written in *Matlab* runned during the post-processing phase. This Matlab script is explained in chapter *Matlab script for the Post-Processing*. In particular, the interrogator at our disposal is constituted by four channels for each fiber optic and it permits us to interrogate 16 sensors for channel with a total of 64 sensors.

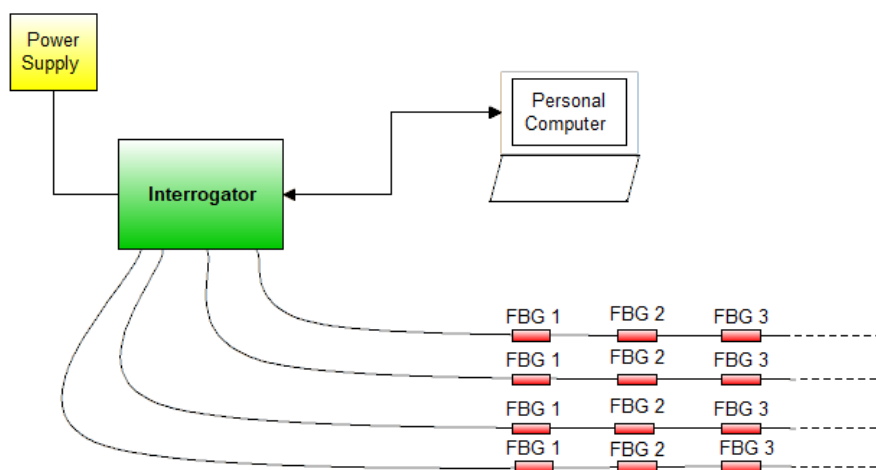


Figure 3.23. Interrogation system

The fiber optics installed on the test bench are Single Mode with a core and cladding diameter of about  $9 \mu m$  and  $125 \mu m$ , respectively. The coating is made by Polyimide (PI). In particular two different type of fiber optic are available to us: Polyimide and Acrylate coated fiber optics. In general, a PI coated fiber are thinner than the second one so they are susceptible to mechanical damage [11]. On the other hand, fiber optics with PI coating are characterised by high temperature resistance [11] so they are suitable for harsh environment with high temperature.

# Chapter 4

## Matlab script for the Post processing

The main aspects of the Matlab script are shown in this chapter. This script is important for the post processing of raw files detected by using the *interrogator*. As written in the previous chapter, by setting the interrogator software, we can directly obtain strain and temperature obtained by the interrogator. However, it has been necessary to write a Matlab script for the post-processing of raw files and to validate the quality of detected and measured data.

### 4.1 Structure of the Matlab script

The Matlab script is based on three macro areas: *Pre-Processing*, *Processing* and *Post-Processing*.

In the first area that is the *Pre-Processing*, user have to insert the file name that he wants to analyse and to set important parameters that are useful during the computation of values of strain and temperature.

During the *Processing* phase, all data contained in *.log* file obtained from the interrogator are organised in data structures and these permit to identify all informations for each sensor. The last step, is the *Post-Processing* that consists on the plot management where user can choose to plot graphs related to a particular channel or sensor. Therefore, by setting a *personalised* analysis it is possible to plot graphs with strain and/or strain with temperature compensation. Regarding to the processing phase, it is not shown to user but it is processed by the calculator.

## 4.2 Basic physical principle

The Matlab script permits to manage n-input channels containing n-FBG sensors, even if the interrogator used by us permits to manage only four channel with sixteen sensors for each channel. The main negative aspect is that it is not possible to manage detected data in real-time. For this reason, the applicability of this script is to analyse the status health of a structure at a later stage. However, a real-time monitoring has been not necessary for our mechanical tests, due to several error sources that affect negatively the quality of measurements. To obtain values of strain, the wavelength variations detected by the interrogator are fundamental and by using the equation 4.1 it is possible to calculate the values of strain [10]:

$$\varepsilon = \frac{\Delta\lambda_B}{(1 - P_e)\lambda_B} \quad (4.1)$$

Where  $P_e$  is the photoelasticity constant. Therefore, usually it is given the gauge factor  $K$  expressed as follows:

$$K = 1 - P_e \quad (4.2)$$

For our applications its value is  $0.78$ . For the strain measurements, it could be necessary to perform a compensation in temperature. Nowadays, many techniques are used. The basic idea for a compensation it is to substract the temperature effects, in terms of wavelength shifts, from a given strain mesaurement.

Strain and/or temperature values are indirectly calculate from wavelegth values detected by the interrogator, even if the interrogator can calculate those physical quantities but it is preferable to process the data.

## 4.3 Explanation of Matlab script

In the following paragraphs are explained the adopted strategies, programming logic and all checks take account during the programming phase.

### 4.3.1 Check of the presence of necessary files

The Matlab script checks if in the directory there are all files with extension *.m* that are necessary for the correct operation of Matlab script. If some files misses, a warning message is shown to the user with a list of missed files. Hence, the user have to check these files and locate them in the directory.

Then, the Matlab script permits to user to write the name of *.log* file that the user wants analyse. This file, as written above, is the output file obtained by the interrogator. The script verifies the presence of this file inside the directory where the Matlab script is located. The name of file has to be written with its extension and with its original name. If the code does not find that file, it will report to user the non-existence of the file and invite the user to re-write it, correctly. After having checked the existence of *.log* file, user can choose to write a note to add to final output file.

### 4.3.2 Choice of analysis type

There is the possibility to choose a *Standard* or *Personalised* analysis. By choosing to execute a *standard analysis*, user can not change no parameter and it carries out to plot graphs of physical quantities detected by the interrogator. On the other hand, if a *personalised analysis* is chosen, user can set manually the physical parameters that are fundamental to calculate analytical strain values. Therefore, in this type of analysis, user can set manually the correlation of a strain sensor related to a temperature sensor, when a temperature compensation is necessary. At the end, a summary is shown to the user and it shows each sensor differentiated in compliance with the type of sensor and a summary of imported data is shown.

### 4.3.3 Setting of FBG sensor

Physical quantities of fiber optic are shown and user can change, in a given range of values, these quantities in respect of fiber optic used. This area of Matlab script is shown only if user choose to execute a *personalised* analysis. The Matlab script takes into account each sensor type *Wavelength* and user has to define if that sensor is a strain or temperature sensor. The correlation of a temperature sensor to strain sensor is fundamental to perform a temperature compensation, because the temperature could shifts the center wavelength of a given FBG sensor.

However, user can not perform this compensation if it is not necessary. Many techniques exist to delete temperature effect on strain measurement and, for example, it is possible to locate a temperature sensor without mechanical strain ( $\Delta\varepsilon=0$ ) in parallel near to the strain sensor. Hence, by subtracting the shifts of wavelength of temperature sensor from to wavelength detected by strain sensor, we obtain a pure mechanical strain. Regarding to nominal wavelength of each sensor, the user can choose to write it manually or, eventually, the Matlab script can do it automatically. With the second choice, the script takes the first wavelength value detected by the

interrogator and present in the *.log* file. Moreover, this automatic inserting of nominal wavelength has been implemented to make quicker the processing of data of a given *.log* file and because it was very difficult to find precisely the correct nominal wavelength. Moreover, if you want to show the preload condition applied on fiber optic, you have to write manually the nominal wavelength indicated on datasheet of the FBG sensor.

Regarding to temperature compensation, the Matlab script permits us to associate a single temperature sensor to an entire sensors group or a single sensor.

At the end of the temperature correlation, a check for the correct thermal correlation is performed; the data structure builded before is analysed by the Matlab script and a further confirm about the correct correlations is request to the user.

#### **4.3.4 Saving data**

This part of Matlab script saves a folder inside the directory automatically. In this folder all graphs plotted during simulations and a summury file with extension *.txt* are saved. The summary file shows all information take during simulations and eventually also the notes written by the user. Folder name has a common prefix that is name of input file analysed and time of simulation. This permits to avoid to overwrite data in case of several simulations of the same input file.

# Chapter 5

## Tests and Measurements

By using the acquisition system at our disposal and the Matlab script for post-processing explained in the previous chapter, it was possible to measure the variations in terms of wavelength and calculate the strain variations. All measurements were carried out by means of a very precise logic; In fact, it is a continuous acquisition over time that is subdivided into ten seconds in which there are ten seconds of static measurements at the step commanded in terms of  $\Delta L$  [mm] with the micro translation stage and ten seconds of transient in which the operator moves the micro translation stage to the next commanded step and so on. This alternation of static and transient measurements continues until the end of that given test. The different measurement campaigns allowed us to study the FBGs and the quality and performances of the locking systems designed by us. This chapter presents the most important results obtained for each locking system. As explained in the chapter "*Assembly of Test bench*", different types of locking systems have been designed and manufactured for the mechanical tests. The first system contemplates the use of a rubber (hard/soft) layer and the second and third one are designed for gluing optical fibers directly on the locking system itself. In particular, these locking systems are mounted on the breadboard by making different lines that vary in length  $L_o$ : short, intermediate and long line.

With regard to the performed tests, statistical analyses were also done to calculate the corrective coefficient  $K_{corrective}$  that is necessary to correct the measurements affected by errors, due to the negative physical phenomena that will be explained in this chapter. In particular, the main steps for the evaluation of the corrective coefficient will be illustrated by showing some significant graphs and tables with results, but only for the locking system which contemplates the gluing of the fiber through the use of resin, because it is the system that guarantees the best results.

## 5.1 Locking system with Hard rubber layer

Several cases related to the locking system with the hard rubber layer will be shown. Therefore, all critical phenomena related to this type of locking system will be explained by showing some important graphs obtained during the measuring campaigns.

### 5.1.1 Response in terms of strain and wavelength by using the short line $L_o=53.59$ mm

Firs of all, incremental load step tests are performed by using the locking system with hard rubber layer and mounting this system, with the fiber optic, along the short line with initial lenght of  $L_o = 53.59$  mm.  $L_o$  is the initial lenght of the fiber optic. It is important to highlight that it is applied a very slight preload on fiber optic. The preload is important because the fiber optic become reactive to the steps applied by using a micro translation stage. In table 5.1 are shown main properties of this type of test.

Table 5.1. Incremental load step test with hard rubber and  $L_o=53.59$  mm.

| Incremental load step Test |             |                 |
|----------------------------|-------------|-----------------|
| Object                     | Material    | Step value [mm] |
| Step                       |             | 0.15            |
| Coating                    | Polyimide   |                 |
| Layer                      | Hard rubber |                 |
| Bases of locking system    | Aluminium   |                 |

The results in terms of measured strain variations and detected wavelength, is shown in the following figure 5.1. In particular, the legend of this graph indicates a standard name in which *Ch1* indicates the channel of interrogator and *Gr1* indicates the fiber Bragg grating interrogated by the interrogator. The numbers of this standard name varies based on the channel and grating used.

In this test, it is possible to notice that between 0 and about 50 seconds, the controlled steps are well detected. The constant lines represents the controlled steps while the lines with an almost vertical slope are the transients in which the operator moves the micro translation stage to the next commanded step. In this graph, it is possible to notice some negative phenomena related to this locking system with hard rubber layer. The main negative phenomenon is the sliding of the optical

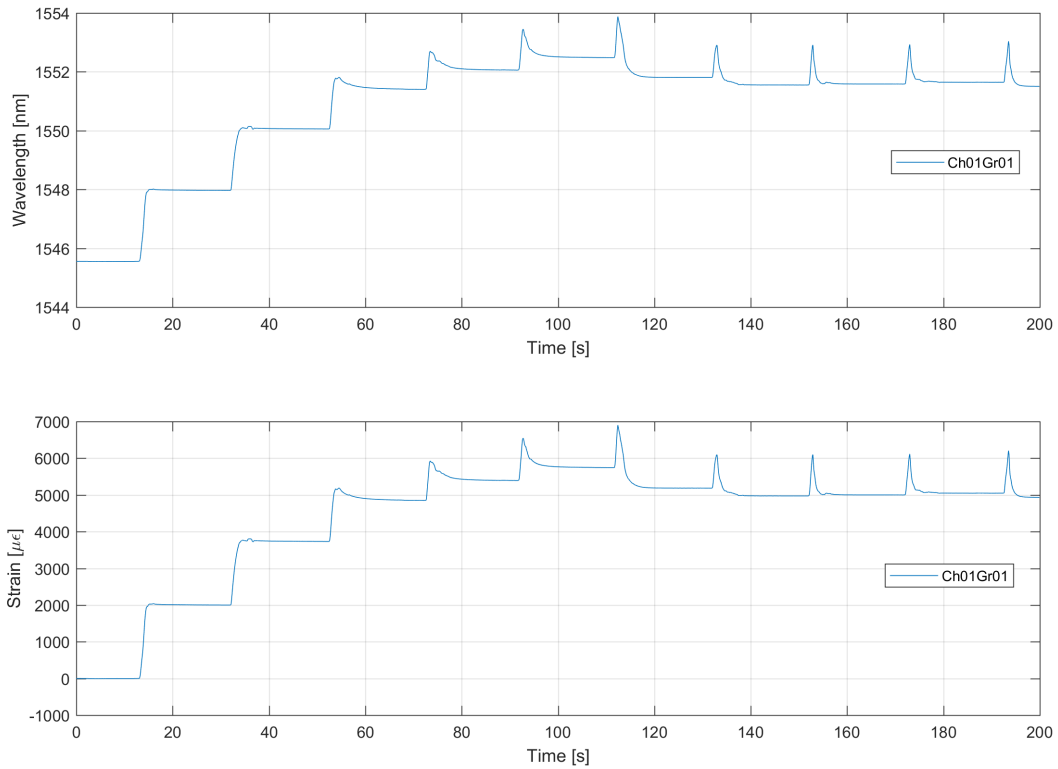


Figure 5.1. Response in terms of strain ( $\epsilon$ ) and wavelength ( $\lambda$ ) for the short line.

fiber on rubber-aluminium interface. In fact, by increasing the controlled load steps, measured strain will be higher and this aspect affects on fiber optic and rubber layer. In particular, it is noted that from 60 seconds to about 110 seconds the optical fiber slides consistently and from about 110 seconds the fiber optic, namely FBG sensor is completely unusable. In addition to the sliding of the optical fiber, there are also two other negative phenomena to be considered, namely the deformation of the rubber layer and the creation of a kind of channel on the rubber itself. This channel is obviously formed because the locking system is designed to press the rubber layer on the fiber, which creates a cavity in the rubber. This channel causes a further sliding of the optical fiber. All these negative phenomena make inaccurate the obtained measurements.

The sliding of the fiber between the rubber-aluminium interface is possible to see in the following figure 5.2. In fact, during the 10 seconds of measuring acquisition, from 60 to 70 seconds, the curve is not fix to a constant value of strain but it change against time because of the sliding of fiber optic and the possible deformation of the rubber layer.

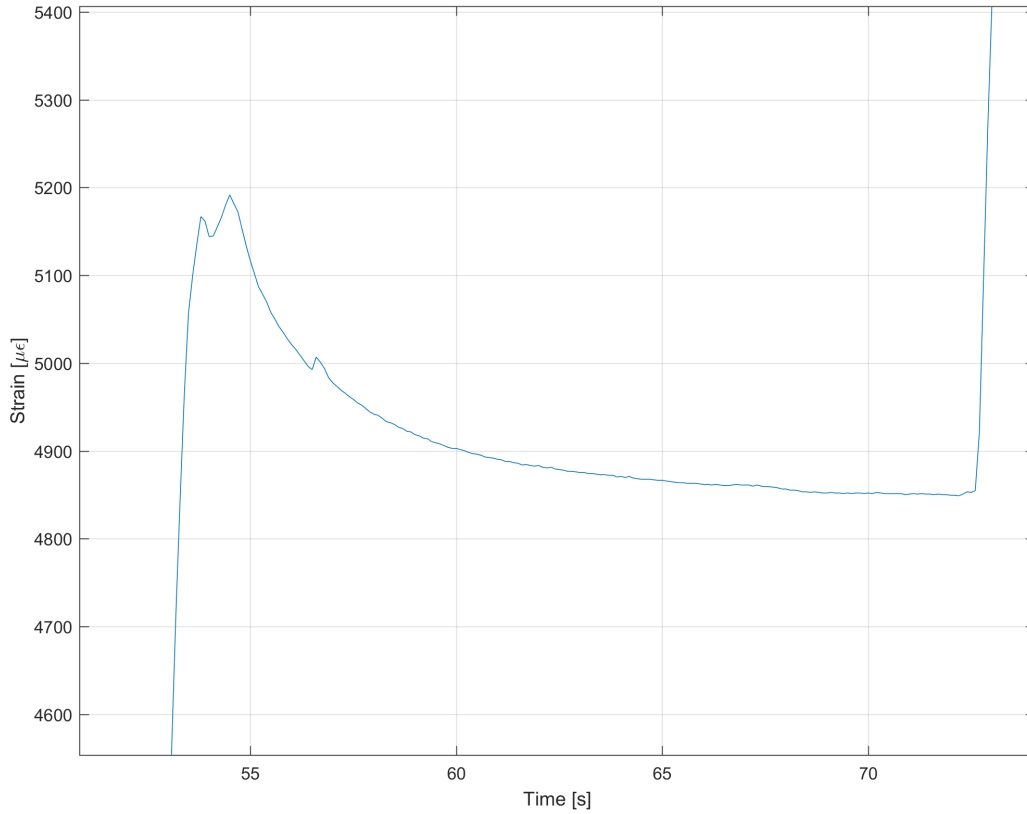


Figure 5.2. Detail of fiber optic sliding in terms of strain for the short line.

As previously written, a statistical analysis was performed for the evaluation of the corrective coefficient of our measurements. From this analysis it is possible to obtain a graph that shows the data fitting and the theoretical curve. Moreover, in this graph especially in case of locking system with rubber, we can see the sliding of the fiber because the experimental curve does not pass through the origin of the axes but intersect the Y-axis. This, as we will see in the following paragraphs, does not happen in case of locking system with epoxy resin.

The procedure to obtain the experimental curve and the average points is shown in the paragraph *Comparison between two concepts of locking systems*.

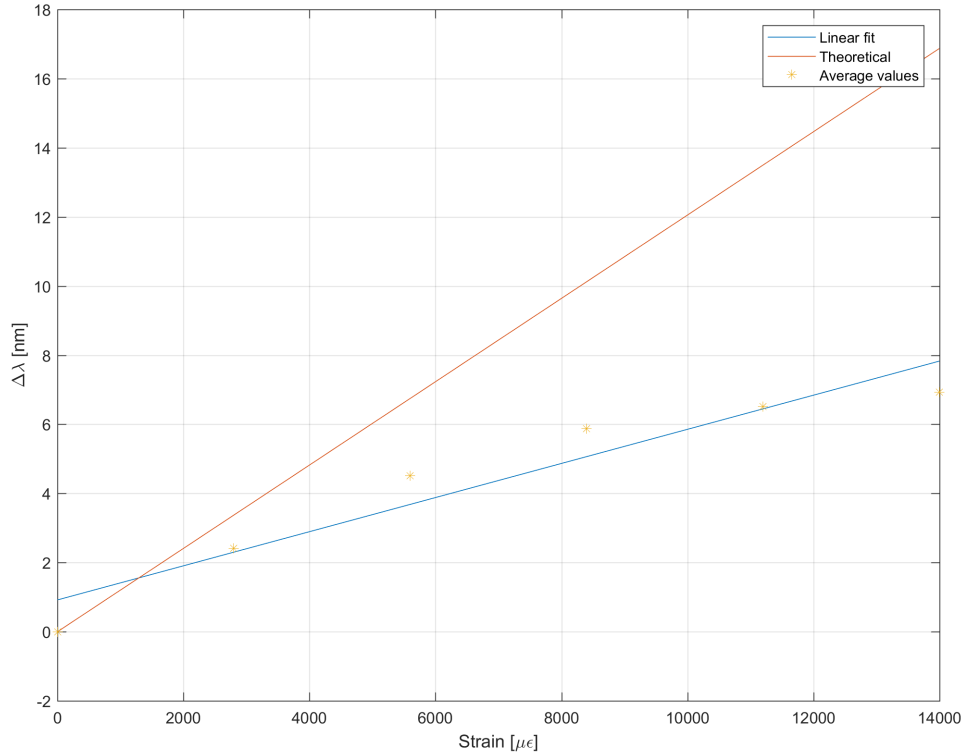


Figure 5.3. Experimental and Theoretical curves for locking system with hard rubber and  $L_o=53.59$  mm.

### 5.1.2 Response in terms of strain and wavelength by using the intermediate line $L_o=128.80$ mm

Regarding to the intermediate line, the response in terms of strain improves clearly. In table 5.2 are shown main properties of this test:

Table 5.2. Incremental load step test with hard rubber and  $L_o=128.80$  mm.

| Incremental load step Test |             |                 |
|----------------------------|-------------|-----------------|
| Object                     | Material    | Step value [mm] |
| Step                       |             | 0.15            |
| Coating                    | Polyimide   |                 |
| Layer                      | Hard rubber |                 |
| Bases of locking system    | Aluminium   |                 |

From the graphs shown in figure 5.4, it is possible to notice how the sliding phenomenon is attenuated. The reason for this behavior compared to the short line illustrated before, is due to the strains that are smaller because  $L_o$  is larger, with

the same commanded steps. From the graphs shown in figure 5.4, it seems that the fiber follows exactly the commanded steps. Instead, plotting the two curves, experimental and theoretical, in terms of  $\Delta L$  [mm], we notice the deviation between these two curves immediately, see figure 5.5.

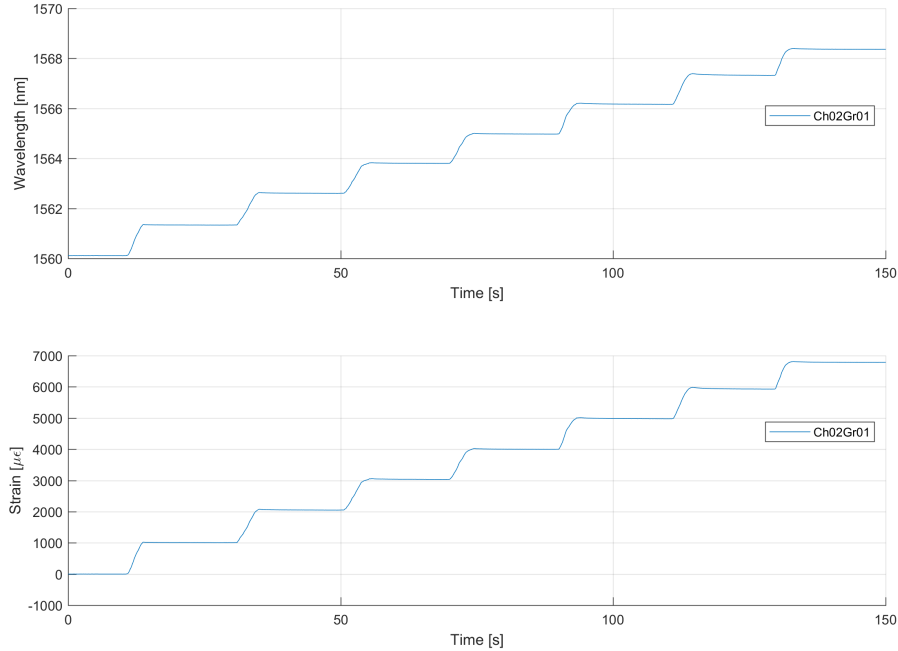


Figure 5.4. Response in terms of strain ( $\epsilon$ ) and wavelength ( $\lambda$ ) for the intermediate line.

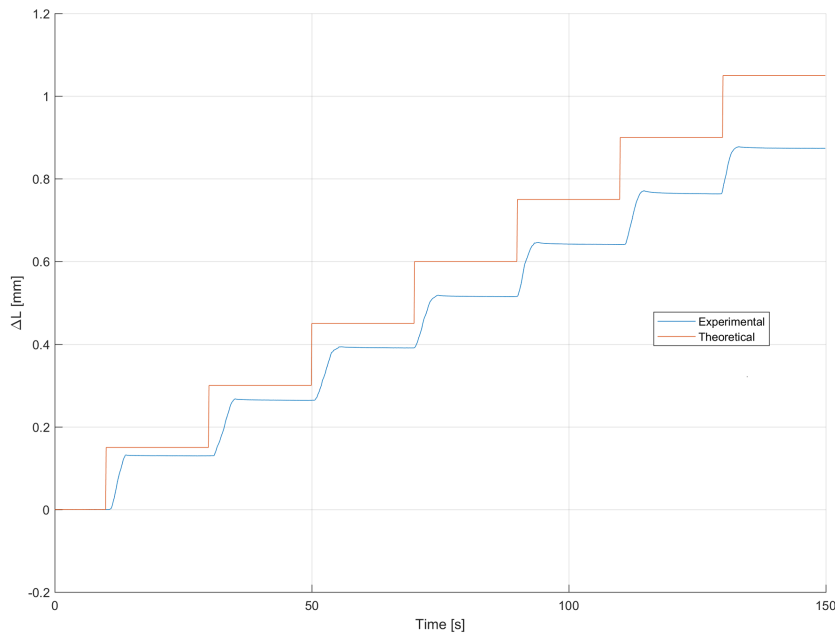


Figure 5.5. Comparison between Theoretical and Experimental curves for the intermediate line.

The gap in terms of  $\Delta L$  that exists over the test is probably due to the rubber deformation and fiber sliding.

However, the sliding is more attenuated with respect to what happened using the short line. To clarify these phenomena it is shown the following figure 5.6 with the detail of a given commanded step:

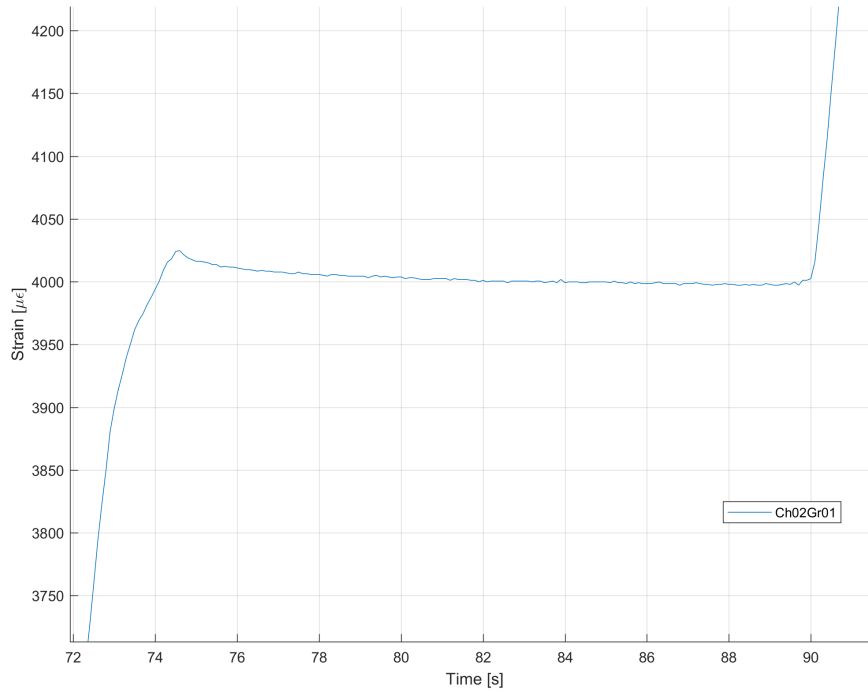


Figure 5.6. Detail of fiber optic sliding and rubber deformation in terms of strain for the intermediate line.

Therefore, once the test is concluded and removing the load, another confirm about the fiber sliding is given observing the shape of fiber optic, see figure 5.7:

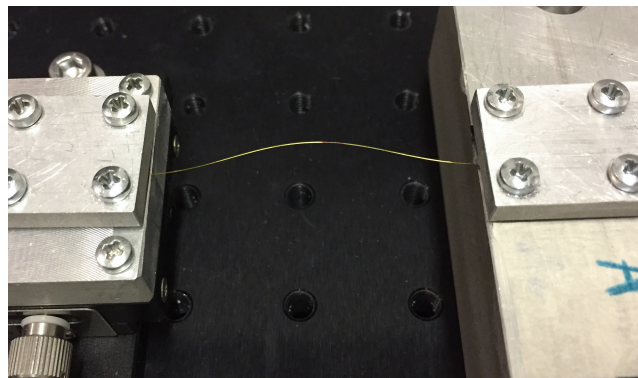


Figure 5.7. Demonstration of fiber sliding by using a locking system with the hard rubber layer.

### 5.1.3 Response in terms of strain and wavelength by using the long line $L_o=228.94$ mm

Regarding to the long line with an initial length of about  $L_o=228.94$  mm, it is possible to notice that its trend is similar to that obtained for the intermediate line. Obviously, strain are smaller compared to the short and intermediate line, because the initial length is larger and the commanded step are the same.

Table 5.3. Incremental load step test with hard rubber and  $L_o=228.94$  mm.

| Incremental load step Test |             |                 |
|----------------------------|-------------|-----------------|
| Object                     | Material    | Step value [mm] |
| Step                       |             | 0.10            |
| Coating                    | Polyimide   |                 |
| Layer                      | Hard rubber |                 |
| Bases of locking system    | Aluminium   |                 |

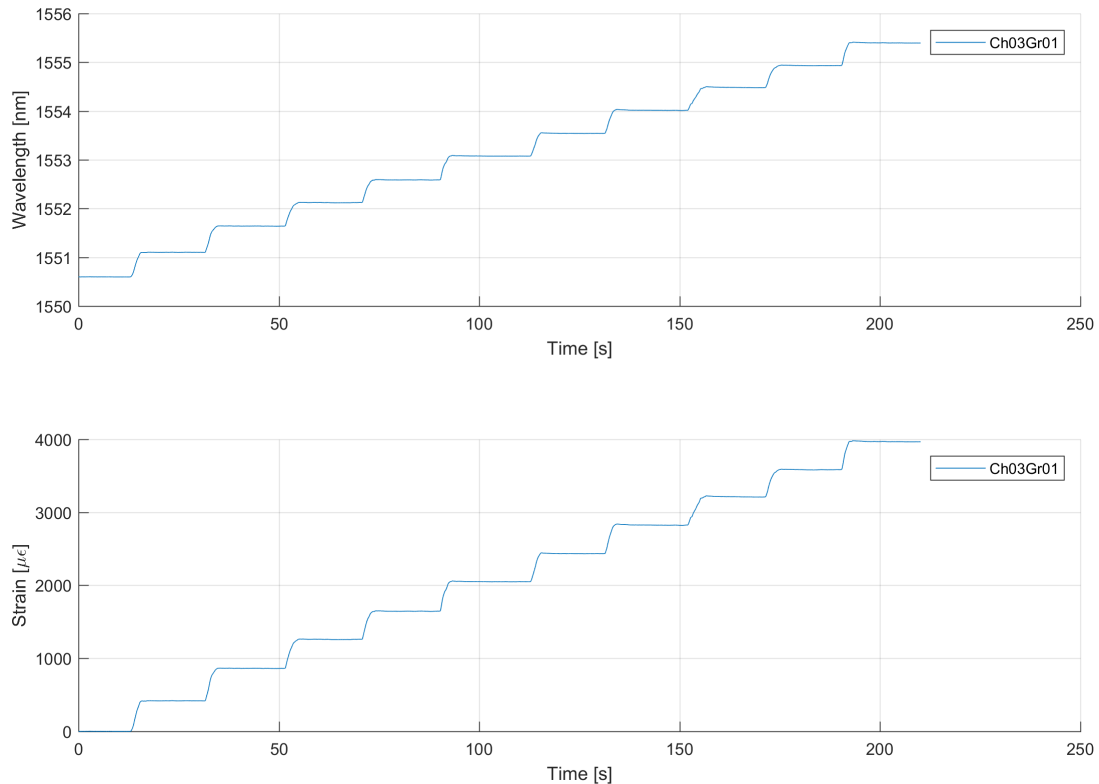


Figure 5.8. Response in terms of strain ( $\epsilon$ ) and wavelength ( $\lambda$ ) for the long line.

Similarly to the previous case, it presents the graph that shows the deviation between the theoretical and experimental curve, see figure 5.9:

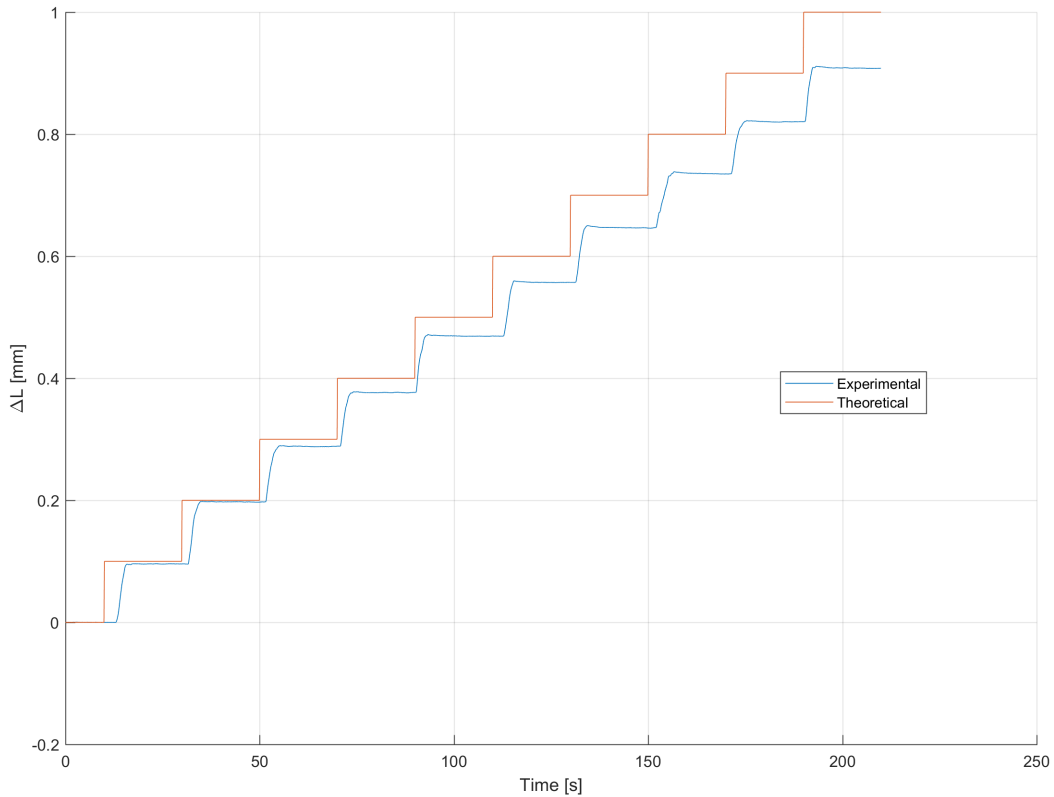


Figure 5.9. Comparison between Theoretical and Experimental curves for the long line.

As previously written, the response obtained is similar to the response of the intermediate line, even if the system responds correctly for the first controlled steps and follows the theoretical curve. However, considering the whole test, it is possible to notice how the gap in terms of  $\Delta L$  continues to grow.

By making a simultaneous test on the three different lines, short, intermediate and long line, it is possible to plot a graph with strain against time. In conclusion, we notice how the short line is the most critical line of the three. The comparison is showed in the figure 5.10.

In particular, the blue curve corresponds to the short line (*Ch01Gr01*), the red curve corresponds to the intermediate line (*Ch02Gr01*) and the yellow curve corresponds to the long line (*Ch03Gr01*).

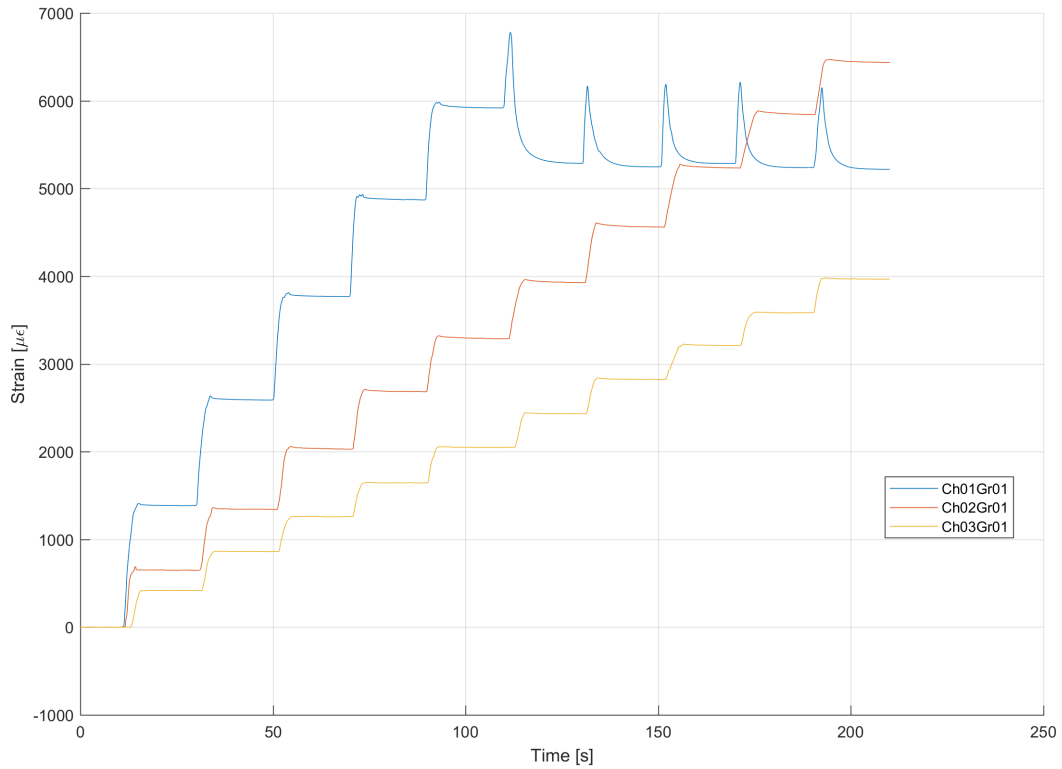


Figure 5.10. Comparison of the response of the short, intermediate and long line in terms of strain.

#### 5.1.4 Repeatability test with locking system with Hard rubber

For locking systems with hard rubber, in addition to performing incremental load step tests, repeatability tests were performed. The table shows the main features of this test:

Table 5.4. Repeatability load step test with hard rubber and  $L_o=228.94$  mm.

| Repeatability load step Test |             |                 |
|------------------------------|-------------|-----------------|
| Object                       | Material    | Step value [mm] |
| Step                         |             | 0.10            |
| Coating                      | Polyimide   |                 |
| Layer                        | Hard rubber |                 |
| Bases of locking system      | Aluminium   |                 |

The result obtained is shown in figure 5.11:

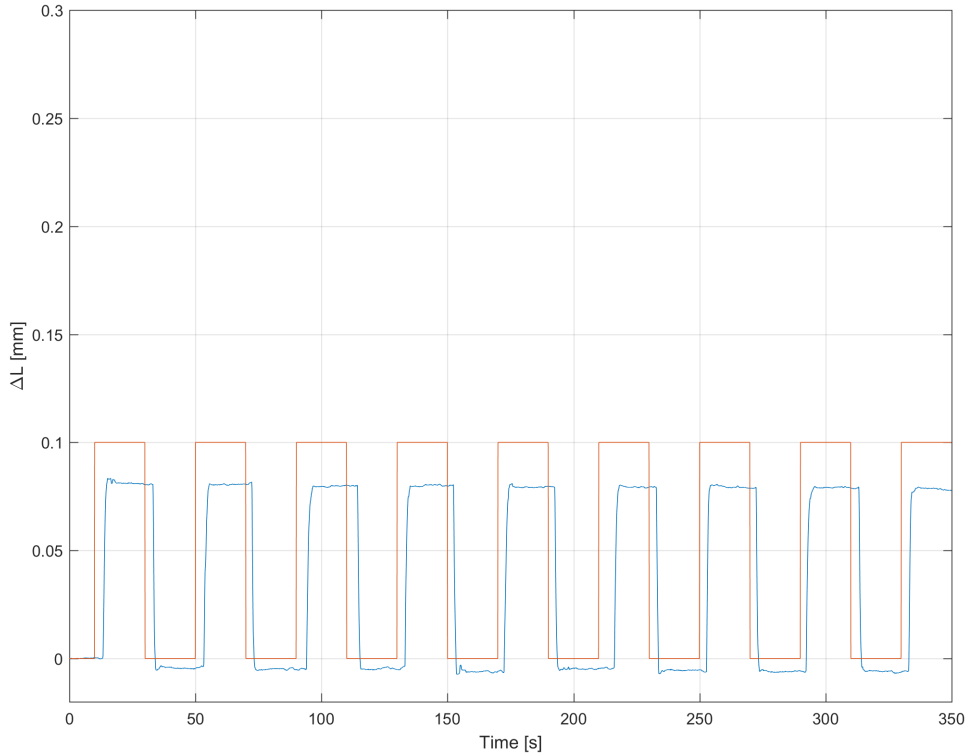


Figure 5.11. Repeatability test with locking system with hard rubber.

The repeatability test are fundamental to test a sensor and to study the performances of locking systems. Moreover, it permits to analyse if sensor is able to provide, by giving the same commanded input, the same measurements that are not very different from each other.

This repeatability test has been performed by using the long line, because it is the one that shows the best results in incremental load step tests. It is possible to notice how the measure is repeatable but there are gaps not acceptable in terms of  $\Delta L$  and that make this locking system not reliable. Therefore in this test, it is clear how the sliding of fiber optic influences the measurements. In fact, when we return to the 0 mm command, rather than returning to this value of command, the detected  $\Delta L$  is minor of zero. To understand this phenomenon is important to highlight that the fiber has been preloaded and since the fiber has slipped on the rubber layer, the preload is lost and the detected wavelength is smaller than the wavelength taken as initial reference ( $\lambda_o$ ).

## 5.2 Locking system with Soft rubber layer

Tests similar to those performed for the locking system with hard rubber, were also performed to test locking systems with soft rubber layer. As done in the previous section about locking system with hard rubber, only the most significant results will be shown. In particular, only the results obtained with the short and the long line are shown. Moreover, the study of this locking system is not explained in detail, because the phenomena are the same of the locking system with hard rubber.

### 5.2.1 Response in terms of strain and wavelength by using the short line $L_o=58.59$ mm and the long line $L_o=228.94$ mm

The first test done is the Incremental load step test. The main properties of this test are shown in the following table 5.5:

Table 5.5. Incremental load step test with soft rubber with  $L_o=58.59$  mm and  $L_o=228.94$  mm.

| Incremental load step Test |                          |                 |
|----------------------------|--------------------------|-----------------|
| Object                     | Material                 | Step value [mm] |
| Step                       |                          | 0.10            |
| Coating Layer              | Polyimide<br>Soft rubber |                 |
| Bases of locking system    | Aluminium                |                 |

The response in terms of wavelength and strain is presented in the following figure 5.12. From this graph it is possible to notice how the fiber is subject to a continuous sliding on the soft rubber.

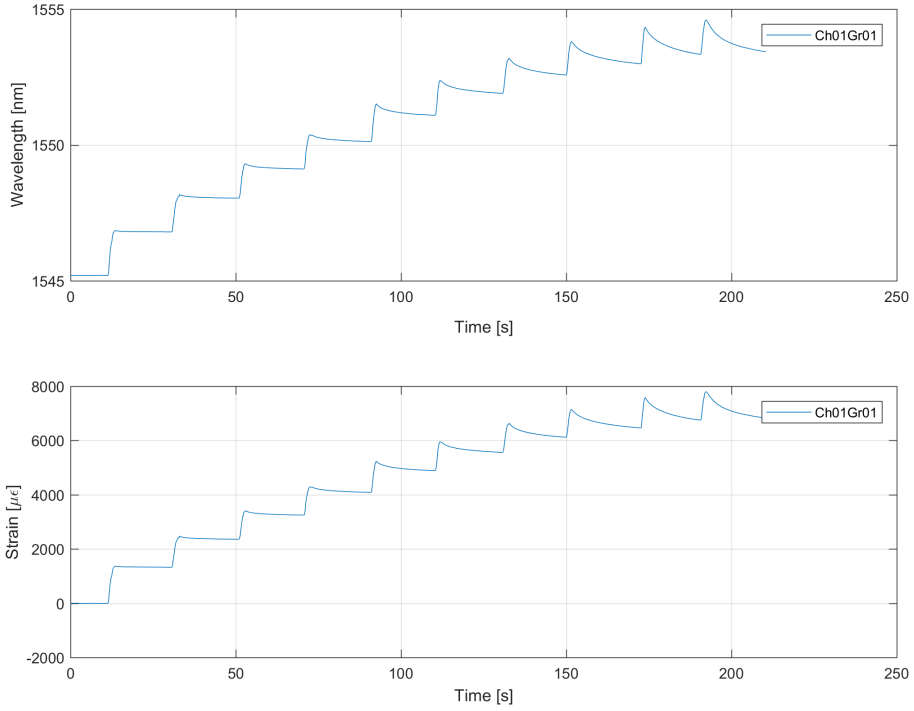


Figure 5.12. Incremental load step test with locking system with soft rubber on short line  $L_o=58.59$  mm.

Regarding to the long line, it has been obtained the following graphs 5.13:

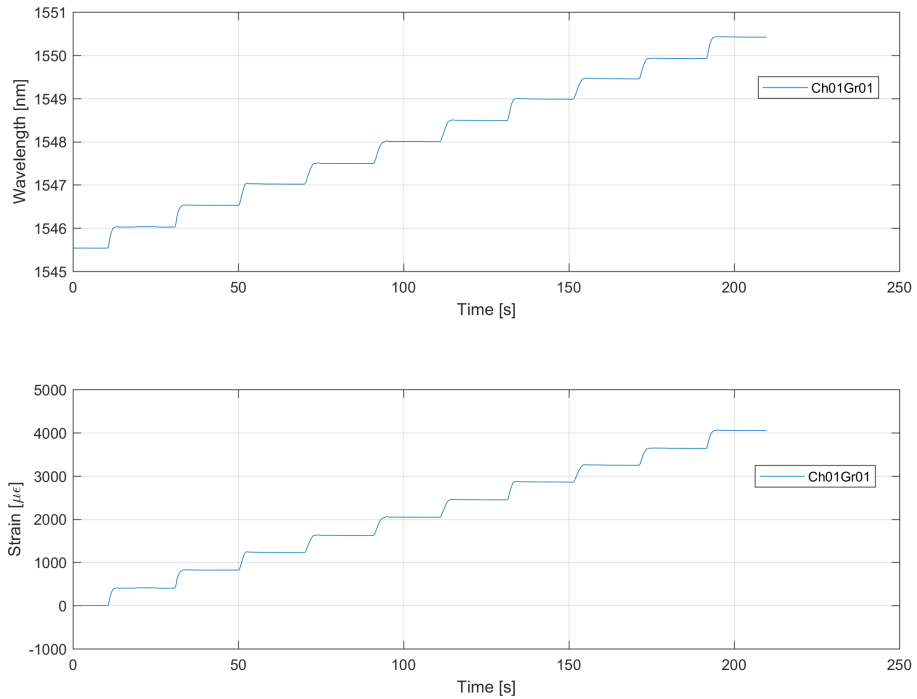


Figure 5.13. Incremental load step test with locking system with soft rubber on short line  $L_o=228.94$  mm.

Also for the long line, the sliding of fiber optic and the deformation of rubber are clear and they are shown in the following figure 5.14:

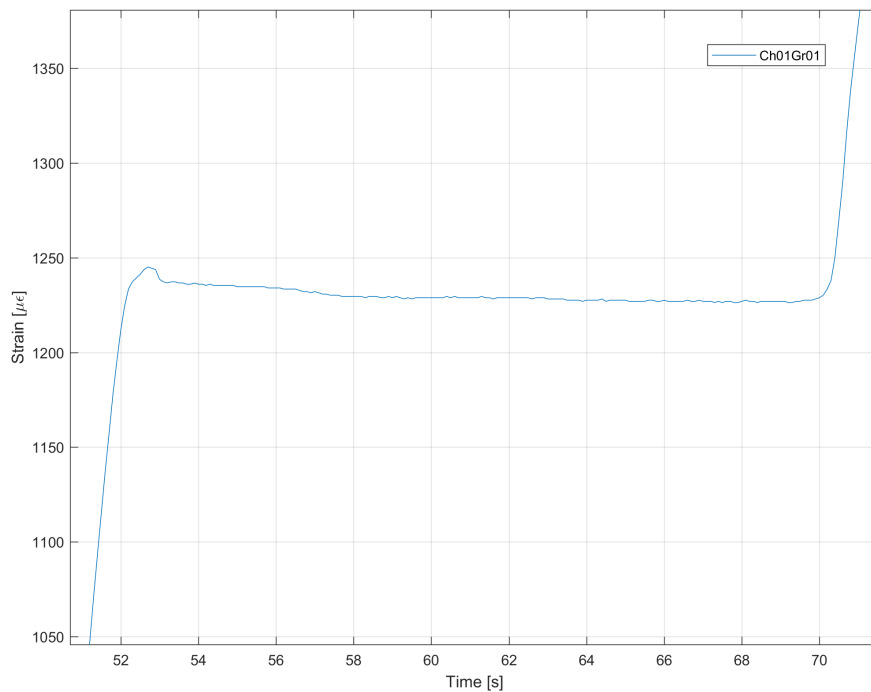


Figure 5.14. Detail of sliding and deformation in terms of strain for the long line.

Also using a soft rubber layer, a cavity created on this layer cause a further sliding of fiber optic. An example of cavity is shown in the following figure 5.15:



Figure 5.15. Cavity of the soft rubber.

The fiber optic, mounted on the long line, seems to respond correctly to the commanded steps. Unfortunately, even if the measurement is repeatable but the sliding of the fiber optic on rubber layer is clear. To study this behaviour, a repeatability test was performed and also in this test a slight preload is applied:

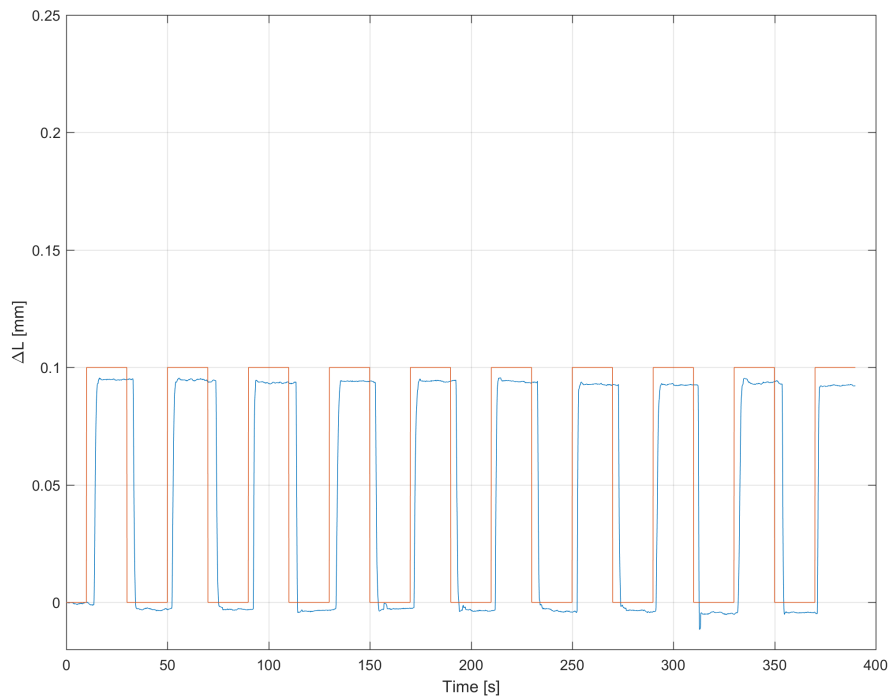


Figure 5.16. Repeatability test with locking system with soft rubber on long line  
 $L_o=228.94$  mm.

### 5.3 Locking system with Epoxy resin

At the end, several mechanical tests have been done by using locking systems manufactured by 3D printing. Hence, a chemical locking is applied to lock fiber optics. Two types of tests such as repeatability and incremental load step tests have been done. Therefore, these tests have been conducted to study the quality and the performances of two concepts of locking systems (explained in chapter *Assembly of Test bench*). The former is the locking system based on containers where to insert the fiber optic ends and cast epoxy resin, while the latter is the locking system based on rectangular plates and the fiber ends are glued on the plates, directly. Then, four different lines are setted on the breadboard: two lines with initial length  $L_o$  of about 53.59 mm and 228.94 mm based on the gluing of fiber optics on rectangular plates and other two lines with initial length  $L_o$  of about 151.16 mm. In particular, these lines of 151.16 mm are used to study the performances of two different concepts of locking systems. In fact, the first line is based on the gluing of fiber optics in the containers and the second one is based on the gluing of fiber on rectangular plates. It is important to highlight that all tests are performed by *preloading* the fiber optic. Due to this, we guarantee to have a responsive FBG sensor.

#### 5.3.1 Comparison between two concepts of locking systems

This measuring campaign starts with the study of response in terms of strain variations by varying locking system. In fact, two lines are mounted in parallel with the same  $L_o$  of about 151.16 mm, but with two different concepts of locking systems for resin. First of all, a repeatability test was performed and the main properties of this test are indicated in the following table 5.6:

Table 5.6. Repeatability load step Test for comparison of two concepts.

| Repeatability load step Test |             |                 |
|------------------------------|-------------|-----------------|
| Object                       | Material    | Step value [mm] |
| Step                         |             | 0.10            |
| Coating                      | Polyimide   |                 |
| Layer                        | Epoxy Resin |                 |
| Bases of locking system      | PLA         |                 |

The results obtained about this repeatability test are shown in figure 5.17. The *Ch01Gr01* is relative to the first channel with the fiber mounted using the locking

system with containers and the *Ch02Gr01* is relative to the other line with locking system based on rectangular plates.

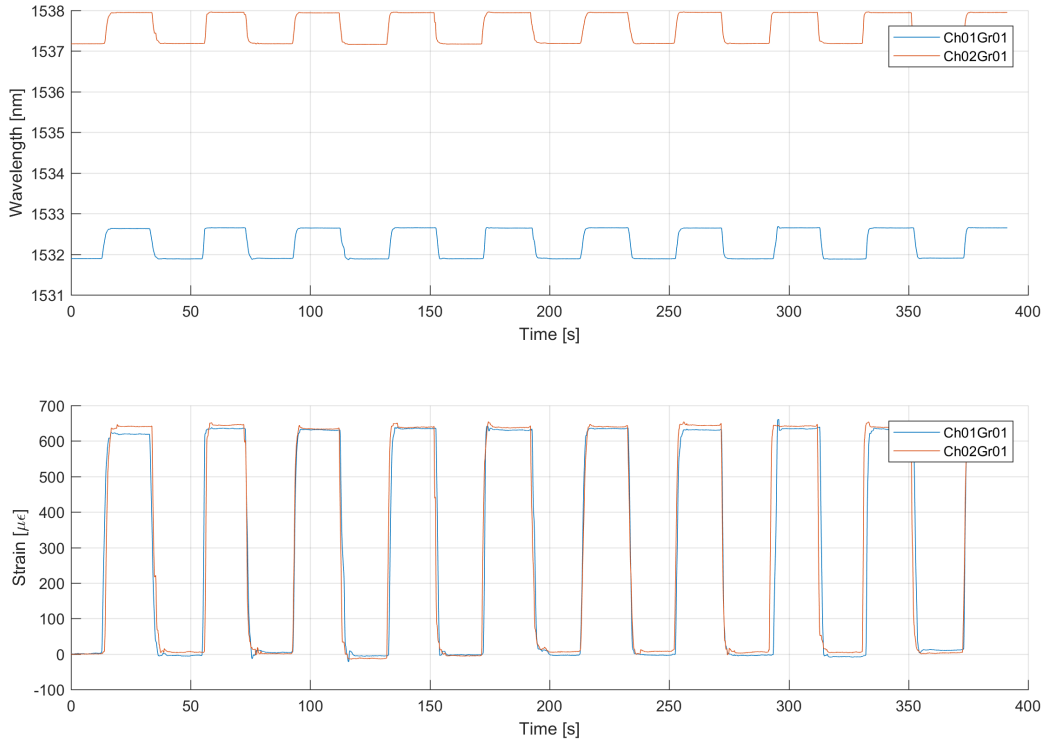


Figure 5.17. Comparison of response by using two different concepts of locking systems.

Therefore, the graph shown in figure 5.18 is about the first channel:

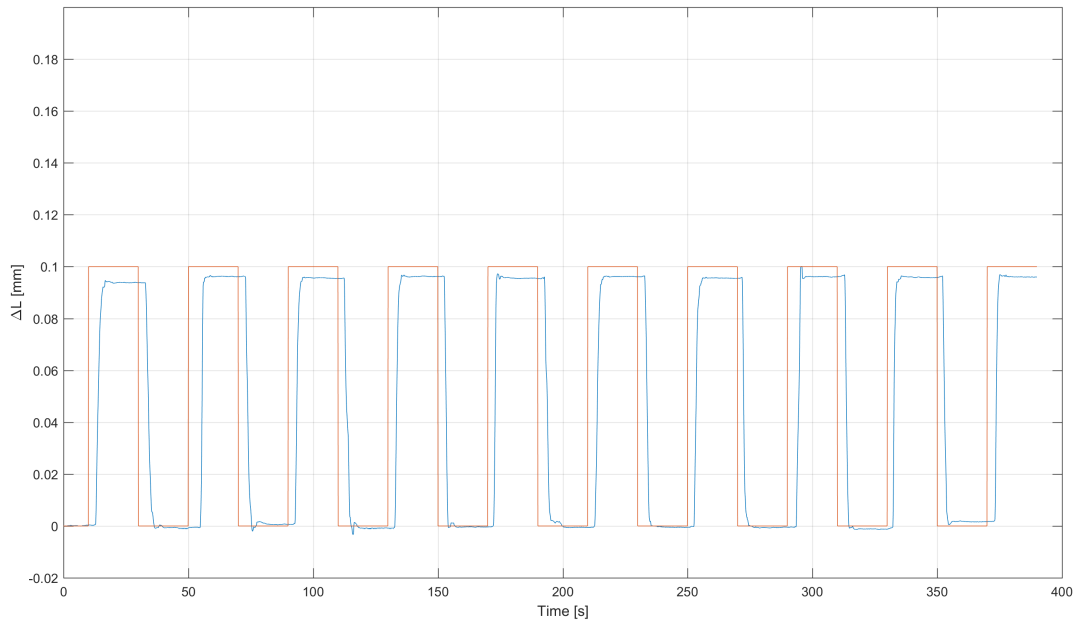


Figure 5.18. Response in terms of  $\Delta L$  [mm] of locking system with containers.

Regarding to the second concept of locking system with rectangular plates, the response is shown in figure 5.19.

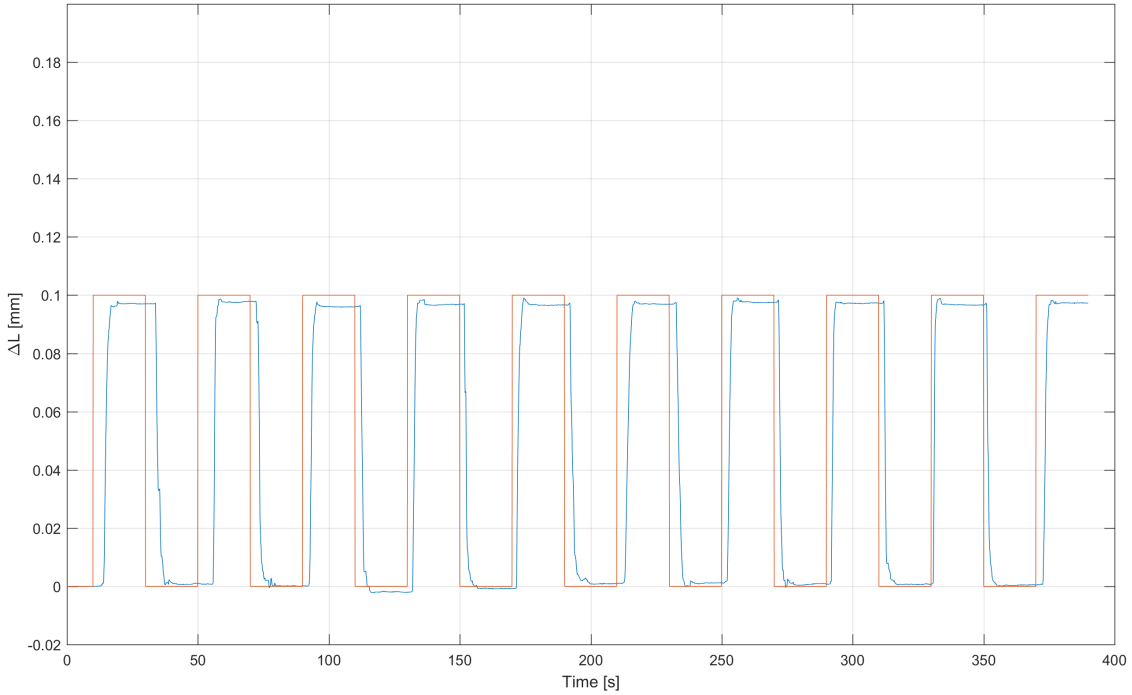


Figure 5.19. Response in terms of  $\Delta L$  [mm] of locking system with rectangular plates.

It is possible to notice how the 0 mm steps are very well detected by sensor. Instead, the 0.1 mm steps are not well detected. Probably, this is due to the deformation of the glue used to lock the fibers and probably to the deformation of the fiber coating. However, these negative phenomena are reversible and it is possible to understand it because removing the applied load the sensor detects 0 mm. This last aspect did not happen with the locking systems with rubber layers. Hence, if the experimental curve (blue line) cannot to reach the command of 0.1 mm, it is due to elastic phenomenon of epoxy resin and/or fiber coating. In fact, the resin can deform itself because of the fiber optic stretching. At the end, it should be noted that sometimes the experimental blue curve does not return to 0 mm because there are negative effects caused by parallax errors and by command given by operator.

For these tests to compare the quality of the two concepts of locking systems and for a numerical evaluation of those negative phenomena explained, the corrective coefficients ( $K_{corrective}$ ) are computed for each test. Obviously, it is necessary to calculate the corrective coefficient to perform a correction of our measurements. Unfortunately, a small number of tests have been performed but they are sufficient to

give a preliminary evaluation of  $K_{mean}$  and the associated error  $\Delta K$ . As performed for locking system with a rubber layer, the corrective coefficient has been computed with incremental load step tests. The properties are shown in the table 5.7:

Table 5.7. Incremental load step test for corrective coefficient.

| Incremental load step Test |             |                 |
|----------------------------|-------------|-----------------|
| Object                     | Material    | Step value [mm] |
| Step                       |             | 0.05            |
| Coating                    | Polyimide   |                 |
| Layer                      | Epoxy Resin |                 |
| Bases of locking system    | PLA         |                 |

As explained previously, the measurements were made following a precise logic, in which ten seconds of measurements to a fix commanded steps are alternated with ten seconds of transient in which the operator takes to the next step. For this reason, the graphs show a step pattern. In order to be able to make a comparison between the theoretical curve and the curve of the fitted data, all the ten seconds blocks related to the transients have been discarded, because they are not important in our analysis. In figure 5.20 are shown all ten seconds blocks of measurements useful for our analyses. In figures 5.21, 5.22, 5.23 and 5.24, it is possible to see the experimental and theoretical curves and how the corrective coefficient acts on the experimental results obtained.

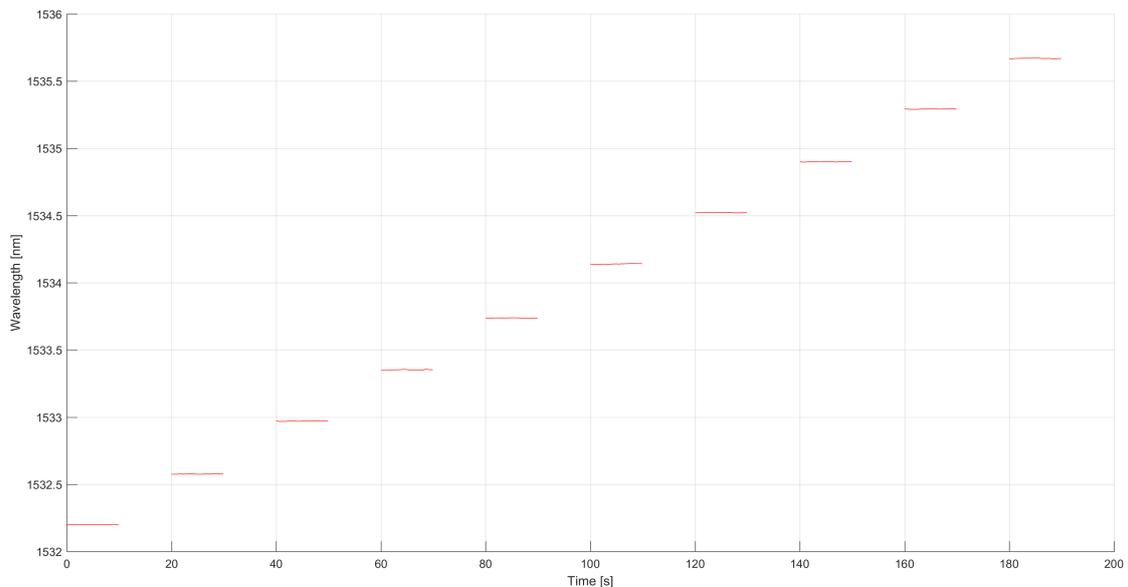


Figure 5.20. Ten seconds blocks of measurements without all transients.

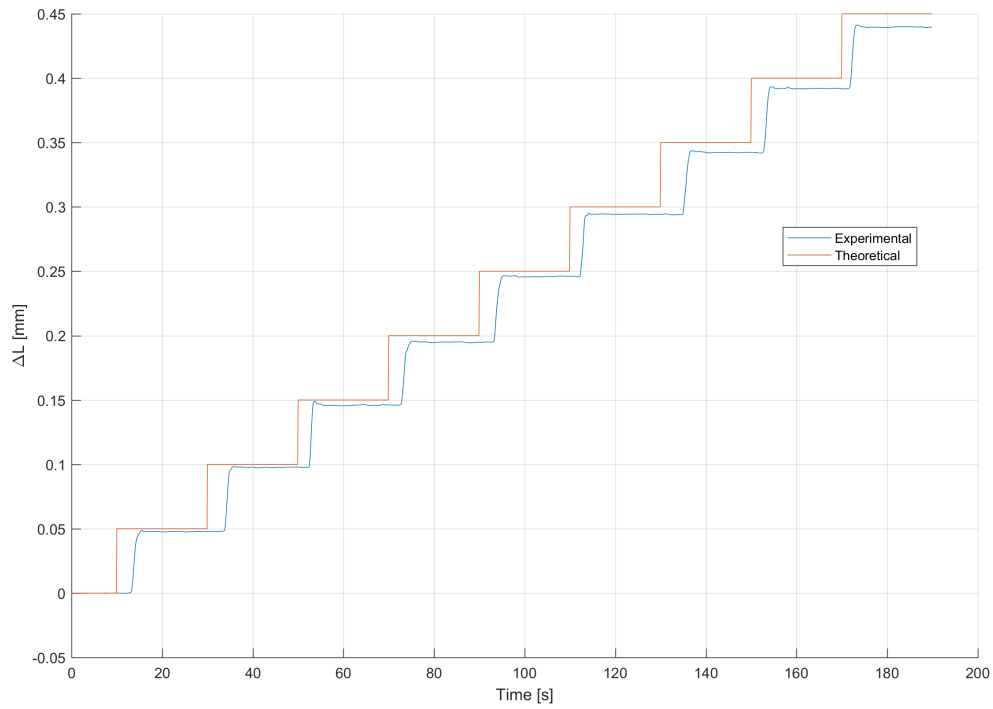


Figure 5.21. Comparison between theoretical and experimental (no corrective coefficient) curves.

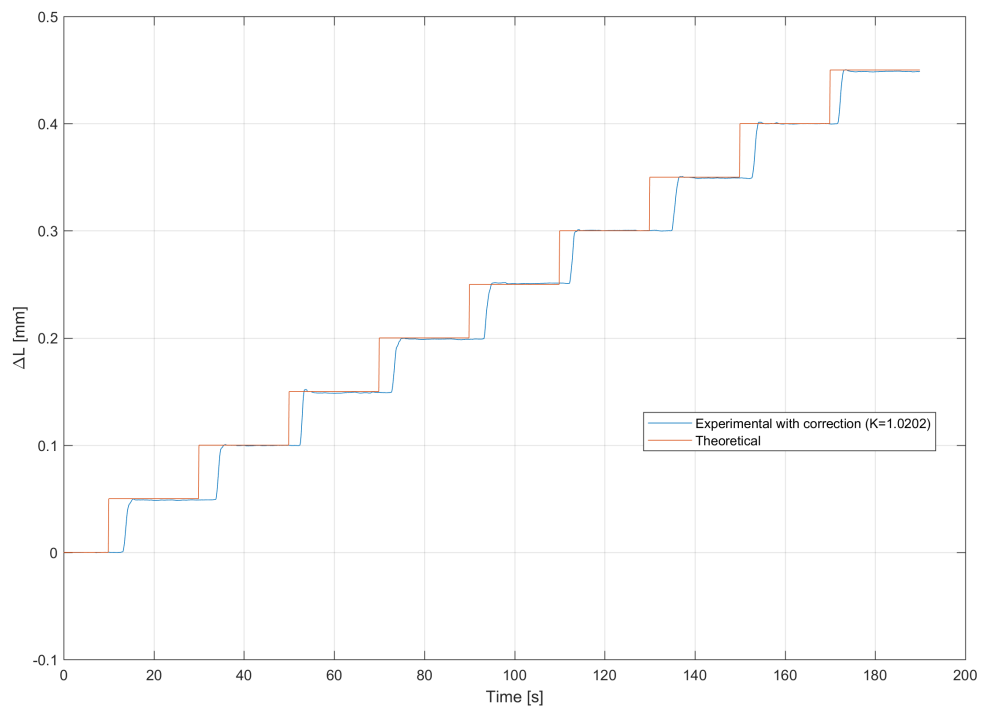


Figure 5.22. Comparison between theoretical and experimental (with corrective coefficient) curves.

Then, other two graphs are obtained:

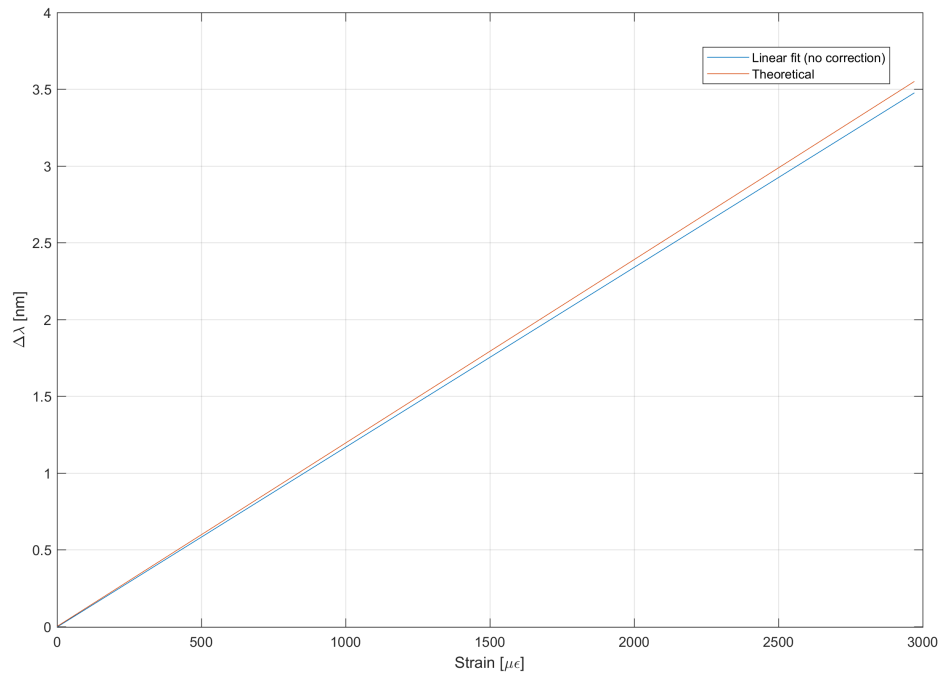


Figure 5.23. Comparison between theoretical and experimental (no corrective coefficient) trend.

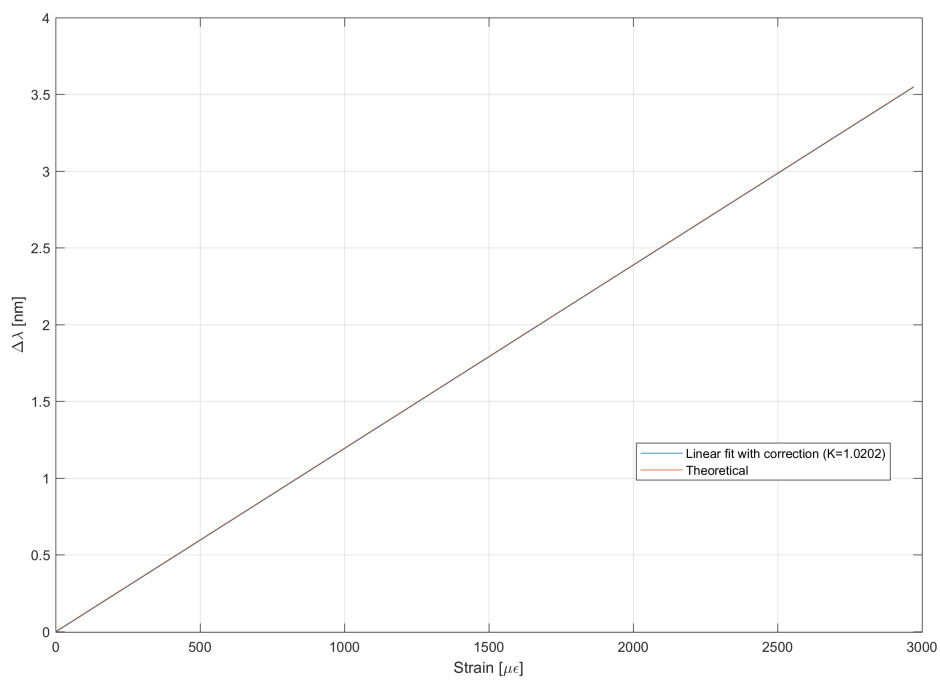


Figure 5.24. Comparison between theoretical and experimental (with corrective coefficient) curves.

The average wavelength values were used to obtain the experimental curves created by using the linear fit, see figure 5.23 and 5.24. Basically, each ten seconds block shown in figure 5.20 contains 100 values of detected wavelengths and each value has to be subtracted from the nominal wavelength. Then, obtained these values subtracted from the nominal wavelength, it is necessary to calculate the average of these values and this average represents a Y coordinate ( $\Delta\lambda$ ), instead the X coordinates are the commands in terms of strain variations applied with the micro translation stage.

As written above, a small number of tests have been performed. In particular, four test per each line have done obtaining a  $K_{corrective}$  per each test. At the end, the mean values and the errors of the corrective coefficients are computed. In the following tables are shown all results get:

Table 5.8. Corrective coefficient values for the first type of locking system.

| <b>Corrective coefficient values</b> |                         |
|--------------------------------------|-------------------------|
| $K_{corrective}$                     | $K_{mean} \pm \Delta K$ |
| 1.0263                               |                         |
| 1.0202                               | 1.0212 $\pm$ 0.0045     |
| 1.0173                               |                         |
| 1.0209                               |                         |

Table 5.9. Corrective coefficient values for the second type of locking system.

| <b>Corrective coefficient values</b> |                         |
|--------------------------------------|-------------------------|
| $K_{corrective}$                     | $K_{mean} \pm \Delta K$ |
| 1.0347                               |                         |
| 1.0359                               | 1.0350 $\pm$ 0.0011     |
| 1.0357                               |                         |
| 1.0337                               |                         |

In  $K_{mean}$  are included all phenomena about deformation of fiber coating and epoxy resin. Instead, the  $\Delta K$  is relative to the errors in command and in particular to parallax error.

### 5.3.2 Conclusion of comparison between two concepts of locking systems

It is possible to notice that there is a little difference in value between two  $K_{mean}$ . In particular, the second type of locking system is characterised by a higher value of  $K_{mean}$ . Probably, it is caused by quantity of epoxy resin used to lock the fiber optics and because when you glue fiber optic on these rectangular plates, you are not sure that fiber is completely surrounded by epoxy resin and a part of the fiber can be directly in touch with the plate. However, it is possible conclude that these two types of locking systems are equivalent and guarantee almost the same response in terms of strain variations. However, it is recommended to do other tests to confirm this hypothesis. Therefore, regarding to the system with rectangular plates it is possible to do further two tests where the first test consists in the gluing of the fiber by using a smaller amount of resin and the second test consists in the creating of a resin layer on plates and then put the fiber on it.

### 5.3.3 Comparison between two different lines: $L_o=53.59$ mm and $L_o=228.94$ mm

To estimate how  $L_o$  can influence measurements, a measuring campaigns were done by using two different fibers glued on two different lines: short and long line. It is important to highlight that the values of  $L_o$  are not standardised and it is due to the mounting of locking systems on the breadboard.

Table 5.10. Incremental load step Test for comparison between two different lines.

| Incremental load step Test |             |            |
|----------------------------|-------------|------------|
| Object                     | Material    | value [mm] |
| Step                       |             | 0.05       |
| Length $L_o$               |             | 53.59      |
| Coating                    | Polyimide   |            |
| Layer                      | Epoxy Resin |            |
| Bases of locking system    | PLA         |            |

Some graphs obtained for the short line are shown in figures below, see figure 5.25, 5.26, 5.27 and 5.28.

By following the same logical process explained before, four tests have been done to obtain four corrective coefficients:

Table 5.11. Corrective coefficient values for the fiber optic mounted on the short line  $L_o=53.59$  mm.

| Corrective coefficient values |                         |
|-------------------------------|-------------------------|
| $K_{corrective}$              | $K_{mean} \pm \Delta K$ |
| 1.1403                        |                         |
| 1.1140                        |                         |
| 1.1180                        | $1.1248 \pm 0.0132$     |
| 1.1270                        |                         |

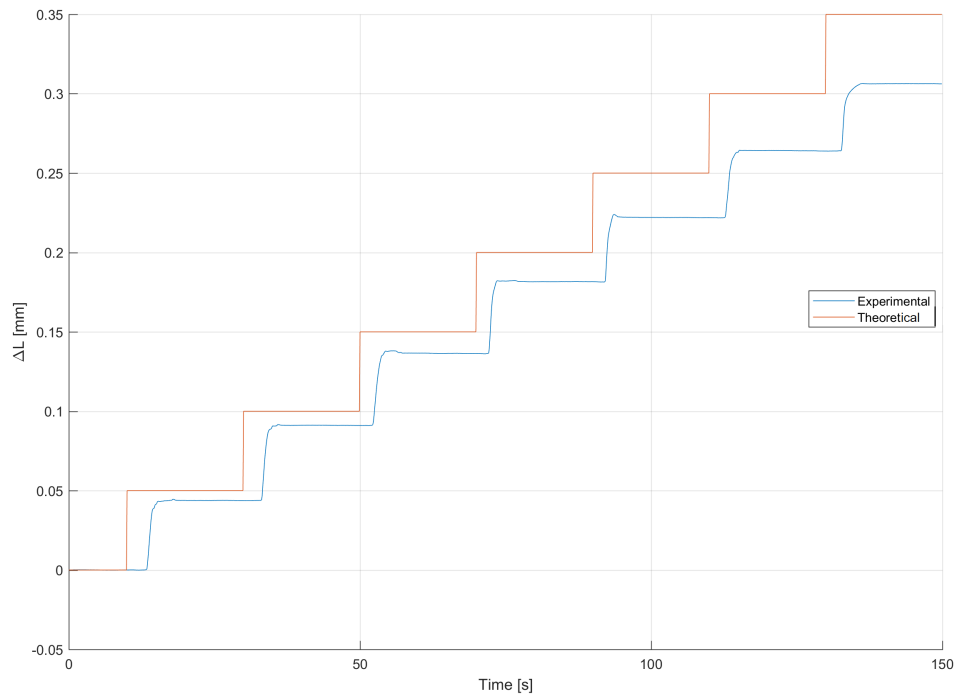


Figure 5.25. Comparison between theoretical and experimental curve by increasing load steps.

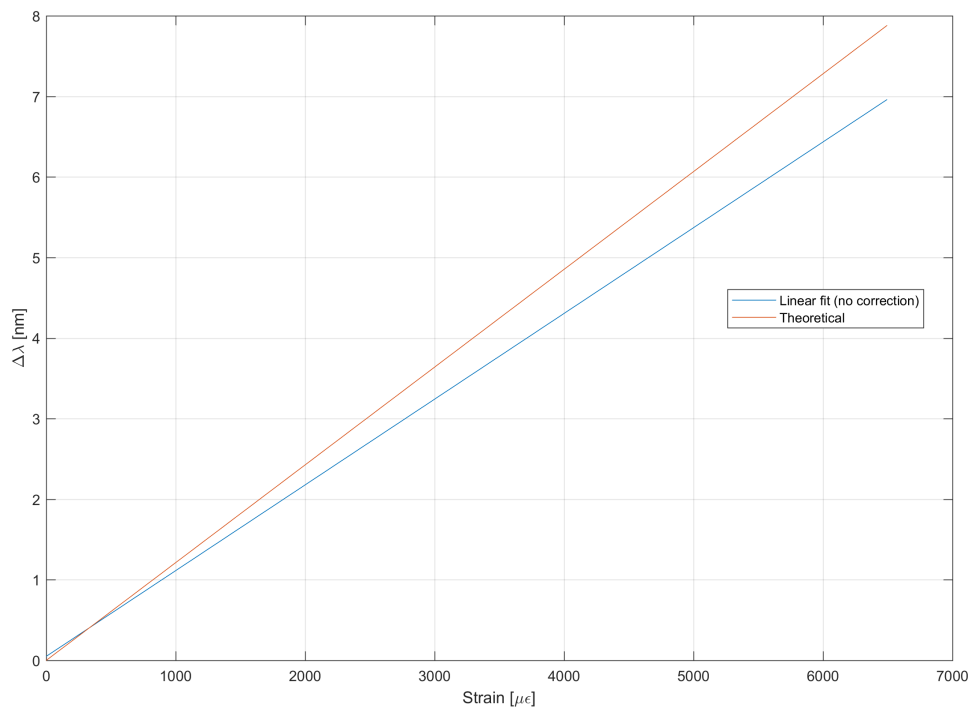


Figure 5.26. Comparison between theoretical curve and experimental curve with linear fit.

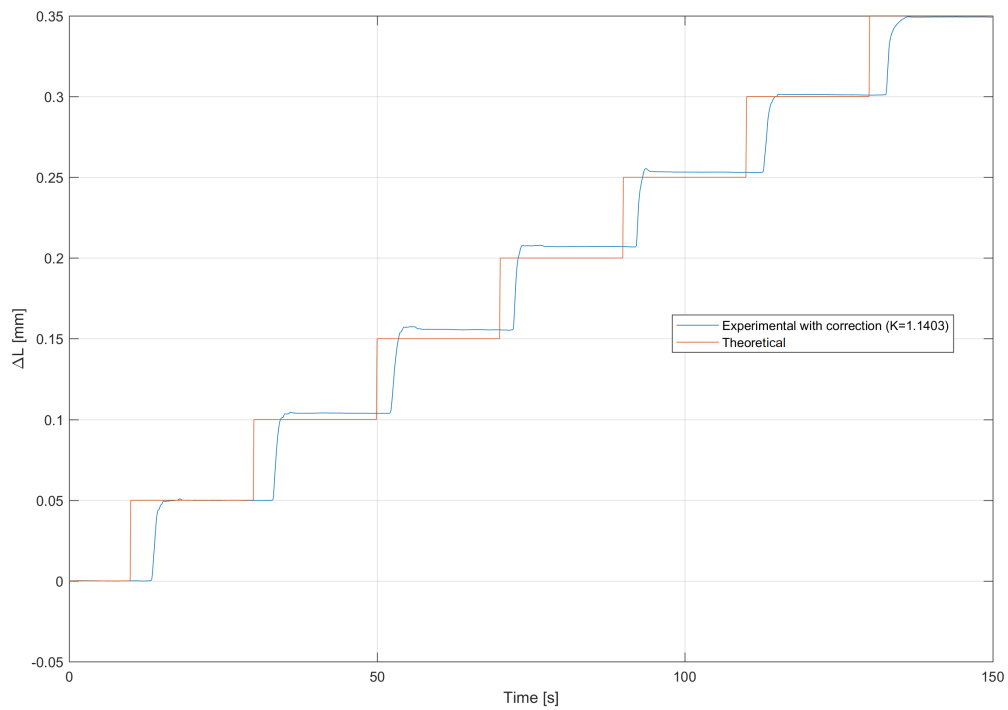


Figure 5.27. Comparison between theoretical curve and experimental curve with correction.

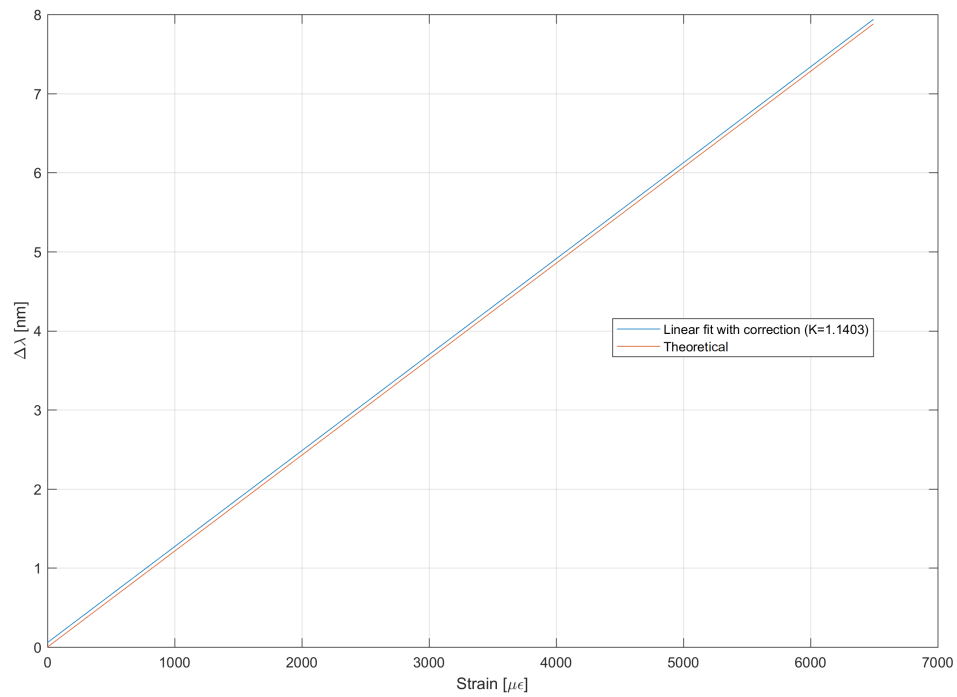


Figure 5.28. Comparison between theoretical curve and experimental curve with correction.

Instead, regarding to the long line:

Table 5.12. Incremental load step Test for comparison.

| <b>Incremental load step Test</b> |             |            |
|-----------------------------------|-------------|------------|
| Object                            | Material    | value [mm] |
| Step                              |             | 0.05       |
| Length $L_o$                      |             | 228.94     |
| Coating                           | Polyimide   |            |
| Layer                             | Epoxy Resin |            |
| Bases of locking system           | PLA         |            |

Also for this long line, four tests have been done to obtain four corrective coefficients:

Table 5.13. Corrective coefficient values for the fiber optic mounted on the long line  $L_o=228.94$  mm.

| <b>Corrective coefficient values</b> |                         |
|--------------------------------------|-------------------------|
| $K_{corrective}$                     | $K_{mean} \pm \Delta K$ |
| 1.0021                               |                         |
| 1.0026                               |                         |
| 1.0002                               | $1.0012 \pm 0.0013$     |
| 1.0000                               |                         |

For a given measurement by using this long line, four graphs are obtained, see figure 5.29, 5.30, 5.31 and 5.32.

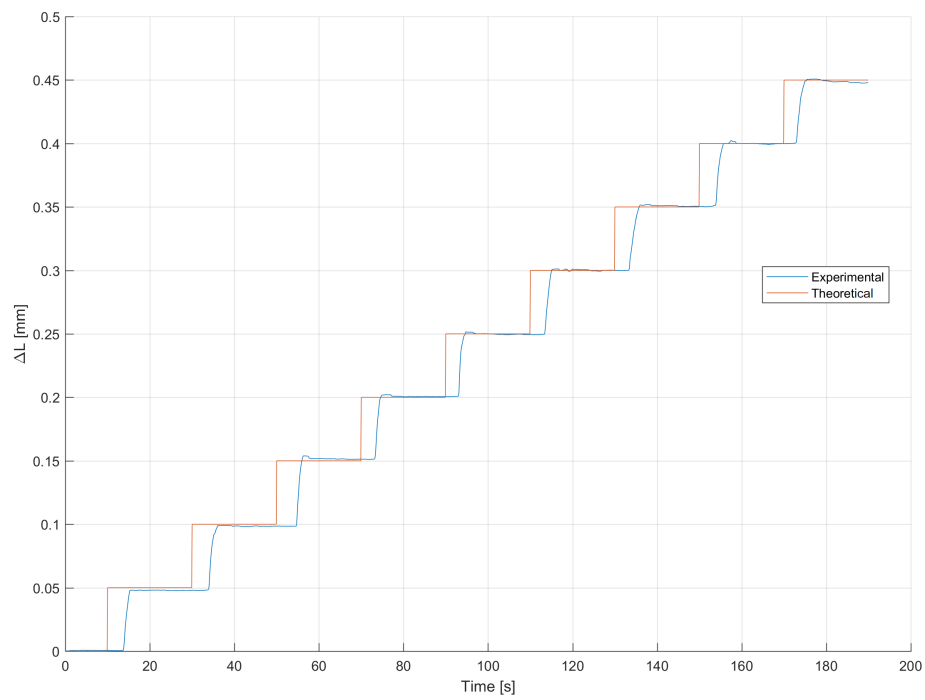


Figure 5.29. Comparison between theoretical and experimental trend by increasing load steps.

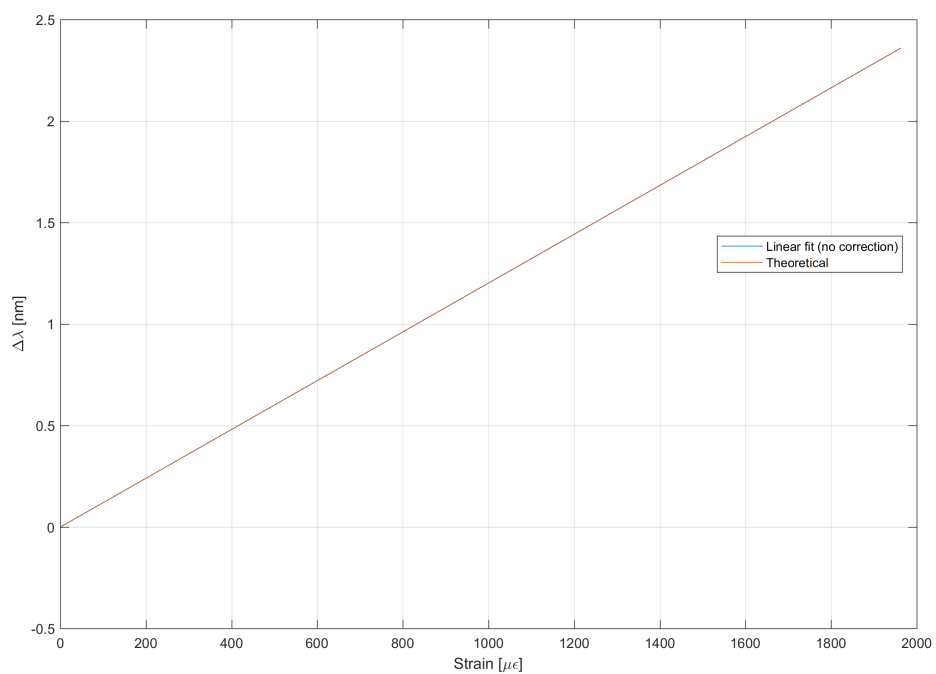


Figure 5.30. Comparison between theoretical and experimental trend with linear fit.

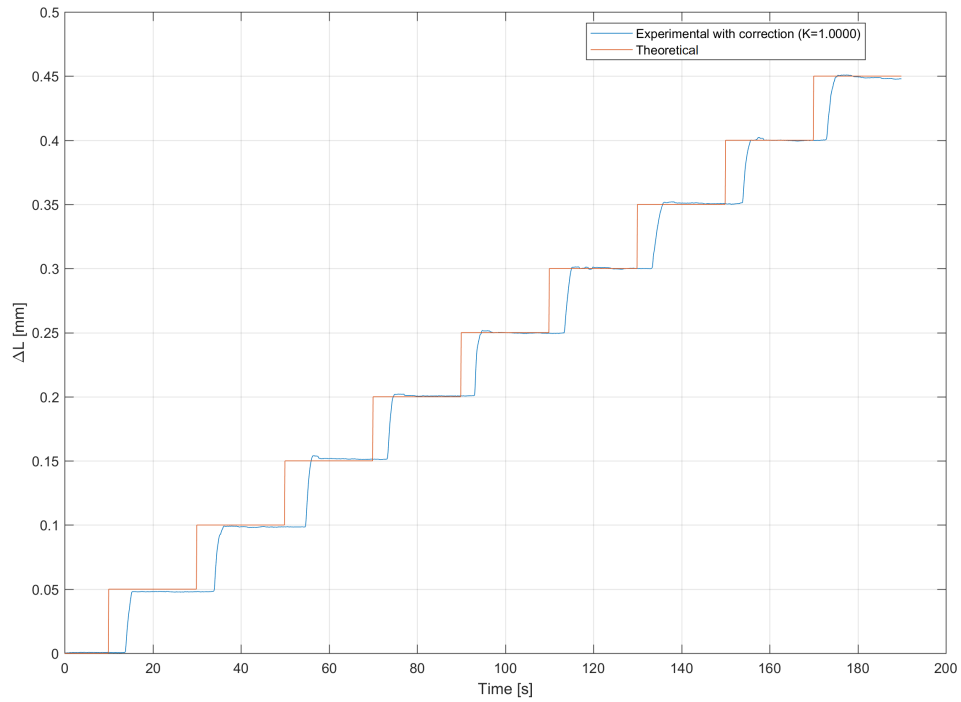


Figure 5.31. Comparison between theoretical and experimental trend with correction.

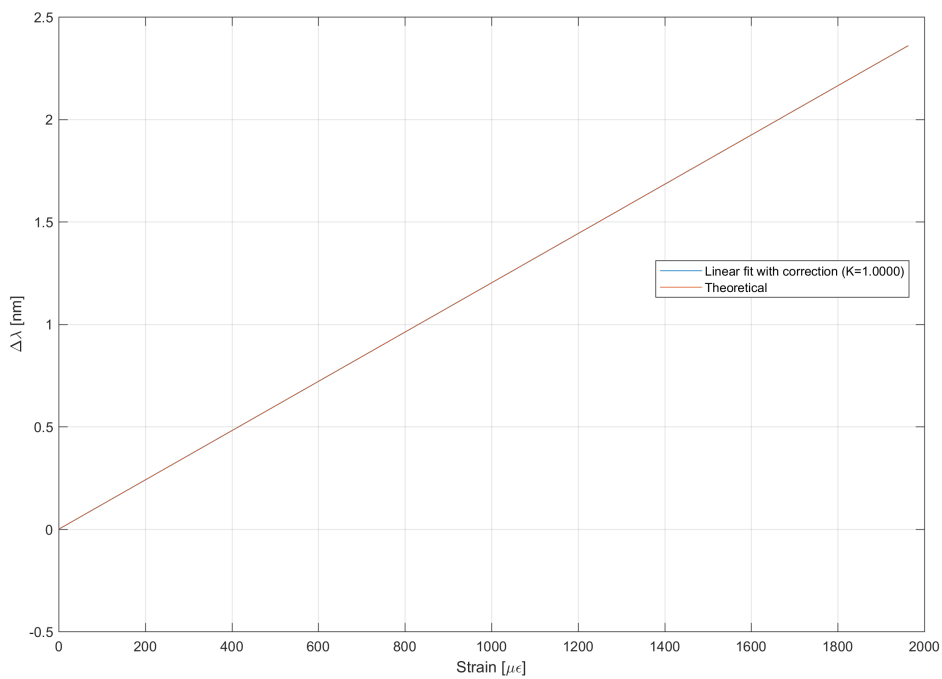


Figure 5.32. Comparison between theoretical and experimental trend with linear fit and correction.

### 5.3.4 Conclusion about the comparison between two different lines $L_o$

According to the performed tests, it is noted that the fiber mounted on a short line presents a critical behavior. This behaviour is due to the application of the load steps to the fiber optic mounted on the line with an initial length  $L_o$  smaller than initial length of the long line. Hence, the strain values are larger. For this reason, the epoxy resin and eventually the fiber coating are more deformed.

It is important to highlight that the same load steps are applied on these two fibers. The best solution turns out to be the system with  $L_o = 228.94$  mm and in general with large  $L_o$  because they guarantee a good response of fiber optic and the best performance of the locking system. Obviously, having the same command and having a larger  $L_o$ , the resin will be subjected to smaller strain.

### 5.3.5 Repeatability Test with long line $L_o=228.94$ mm by varying the preload

To apply a preload on fiber optic is fundamental, because it permits to have a responsive sensor. In our case, the preload is given in terms of  $\Delta L$  [mm] by using the micro translation stage. Focusing on the long line, different repeatability tests are performed and these tests differ from value of applied preload.

The main and common properties of these tests are shown in table 5.14:

Table 5.14. Repeatability load step Test for the long line  $L_o=228.94$  mm.

| <b>Repeatability load step Test</b> |             |            |
|-------------------------------------|-------------|------------|
| Object                              | Material    | value [mm] |
| Step                                |             | 0.10       |
| Length $L_o$                        |             | 228.94     |
| Coating                             | Polyimide   |            |
| Layer                               | Epoxy Resin |            |
| Bases of locking system             | PLA         |            |

In sequence are shown three graphs and each graph is relative to a particular preload condition, see figure 5.33, 5.34 and 5.35.

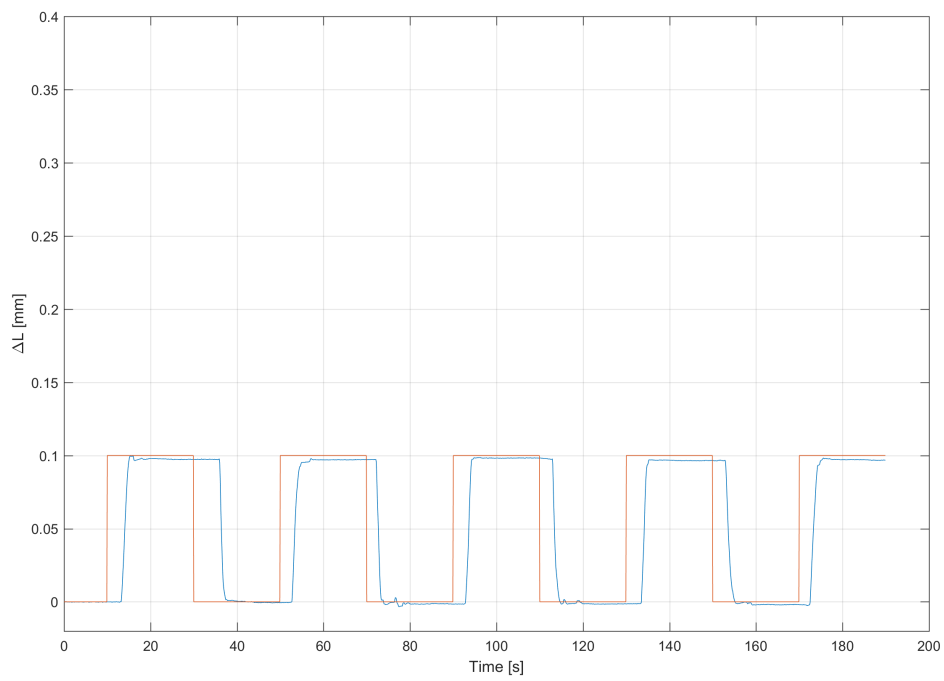


Figure 5.33. Repeatability load step Test by starting with pre-load of 0.30 mm.

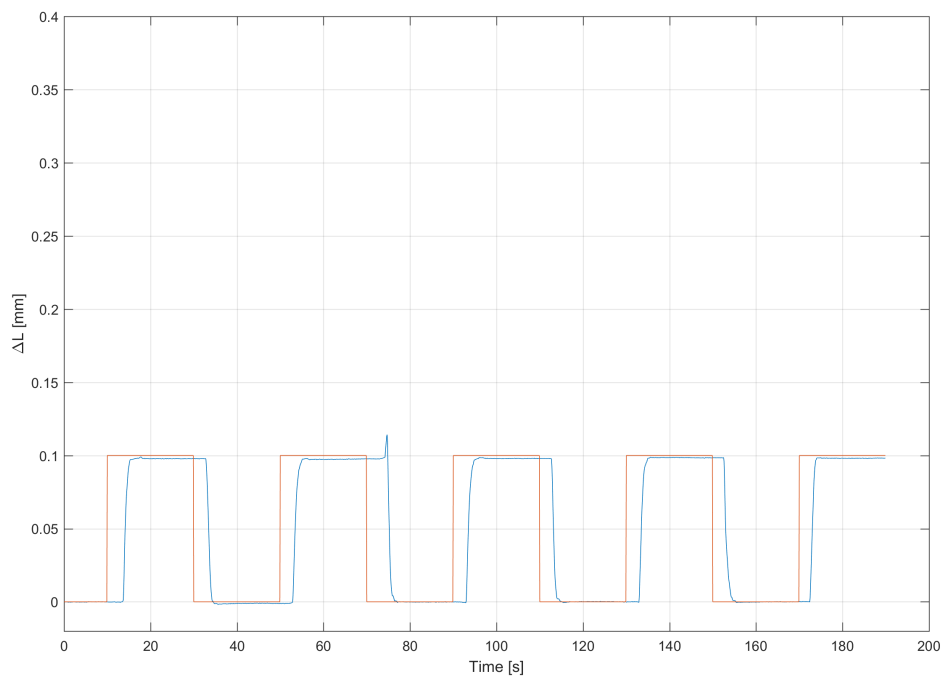


Figure 5.34. Repeatability load step Test by starting with pre-load of 0.20 mm.

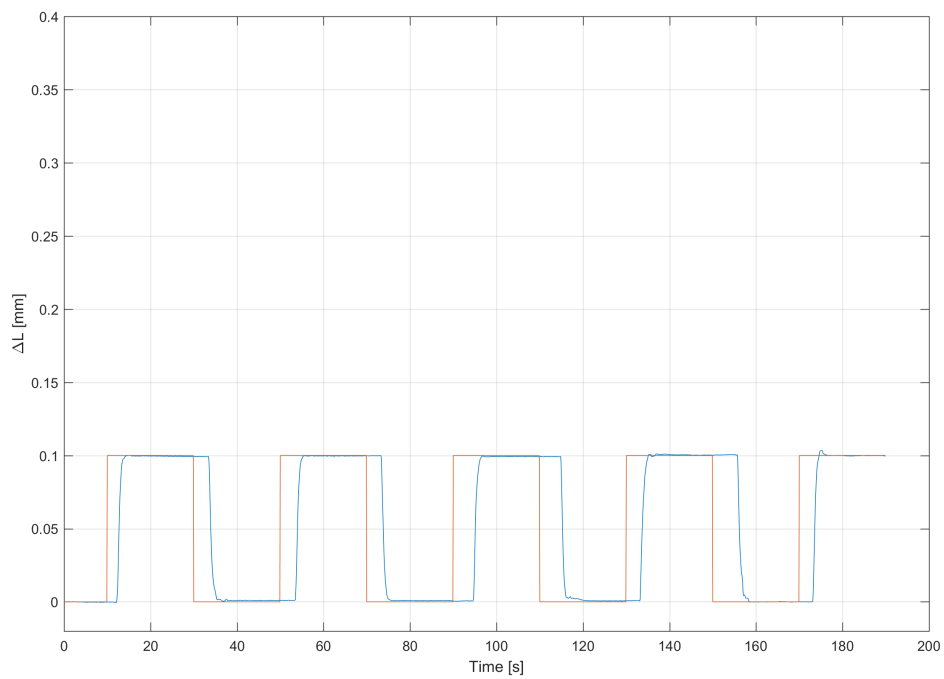


Figure 5.35. Repeatability load step Test by starting with pre-load of 0.10 mm.

It is possible to notice that by reducing the amount of preload, the response in terms of strain variations is better and the experimental curve accurately follow the theoretical curve.

# Chapter 6

## Conclusions and Future works

The main goals of this Thesis are the study of innovative fiber optic sensors, as well as Fiber Bragg Grating sensors and the assembly of a test bench to study the performances of different locking systems. As written in the previous chapters, several locking systems have been designed and they represent a starting point for the future development of these systems for Aerospace applications.

Several measurement campaigns have been done to study the performances of FBG sensors and of designed locking systems. The result is that the systems based on the use of an intermediate rubber layer do not allow the correct operation of sensors making the measurement inaccurate. Moreover, we noticed that by using this type of system the fiber easily slides to the aluminium-rubber interface. For this reason, even if this system is easy to manufacture and assemble and it allows the replacement of the fiber optic in a very brief time, however it does not represent an optimal locking system. Hence, it will not be possible to use it in future tests or applications. On the other hand, the best performing locking systems are those which consider the gluing of the fiber optic. By using this type of locking systems, the most critical phenomenon does not take place, i.e. the sliding of the fiber and consequently the improper operation of the sensor.

For future people who will work on this project, it is advisable to continue the research by using a locking system that involves the gluing of the optical fiber. Moreover, it is advisable to:

- Perform a large number of tests to have more data to obtain more accurate values of corrective coefficients and their errors.
- Perform tests using different fiber optics with different coatings and to use other kind of best-performing resins, to study how these two aspects may

affect the accuracy of the measurements.

- Perform thermal tests by using FBGs as temperature sensors.
- Perform mechanical tests by varying the room temperature to study how it affects the strain measurements.
- Perform mechanical tests by varying the room temperature and then to do the temperature compensation to obtain a pure mechanical strain value.

# References

- [1] R. Kashyap, *Fiber Bragg Gratings, Second Edition (Optics and Photonics Series)* Academic Press, 2009.
- [2] D. Ahuja, D. Parande, “Optical sensors and their applications” in *Journal of Scientific Research and Reviews*, v. 1(5), pp. 060–068, November 2012.
- [3] S. Kumar, M. J. Deen, *Fiber Optic Communications: Fundamentals and Applications* John Wiley and Sons Ltd, 2014.
- [4] Murata, *Handbook of Optical Fibers and Cables, Second Edition* New York, Marcel Dekker.
- [5] G. P. Agrawal, *Fiber-Optic Communications Systems, Third Edition* John Wiley and Sons, 2002.
- [6] M. Yamane, Y. Asahara, *Glasses for photonics* published by the Press Syndicate of the University of Cambridge, 2000.
- [7] B. E. Saleh, M. C. Teich, *Fundamentals of Photonics, Second Edition* John Wiley and Sons, 2007.
- [8] S. Kasap, *Optoelectronics and Photonics: Principles and Practices* Pearson Education Limited, 2013.
- [9] Z. Fang, K. K. Chin, K. C. Ronghui Qu, Haiwen Cai(auth.), *Fundamental of optical fiber sensors* John Wiley and Sons, 2012.
- [10] S. M. Tak, M. K. Kang, D. J. Park, S. S. Lee, “Strain measurement at cantilever beam with fiber Bragg grating sensors and collimators and its correction method” in *International Journal of Modern Physics: Conference Series*, v. 6, pp. 576–582, 2012.
- [11] D. R. Biswas, “Aging behavior of polyimide/acrylate coated optical fibers in harsh environments” in *Optical Engineering*, v. 36, pp. 2169–2170, 1997.